after transfection, core protein levels in the supernatants of all chimeric RNA-transfected cells increased and reached $2.27 \times 10^5$ to $4.93 \times 10^5$ fmol/liter (Fig. 2A and Table 1). Infectivity in the culture medium also increased ($1.61 \times 10^5$ to $3.27 \times 10^5$ FFU/ml) (Table 1), and at this point, most of the cells were core protein positive (Fig. 2B, frame i to l).

As the infectivity of culture supernatant of MA/JFH-1 RNA-transfected cells appeared to increase after long-term culture, we compared viral spread by infection with these supernatants on day 3 (immediately after transfection) and for each peak in core protein levels (after long-term culture). When naïve Huh7.5.1 cells were infected with supernatant on days corresponding to a peak in core protein levels at a multiplicity of infection (MOI) of 0.001, core protein levels in the medium increased rapidly and reached $0.64 \times 10^6$ to $1.13 \times 10^6$ fmol/liter by day 15 after infection (Fig. 2C). Immunostained images showed that most cells were HCV core protein positive on day 15 (Fig. 2D). When naïve Huh7.5.1 cells were infected with supernatant from day 3 at an MOI of 0.001, core protein levels in the medium did not increase under these conditions (Fig. 2C). These results indicate that both MA/JFH-1 chimeric viruses (MA/JFH-1.1 and MA/JFH-1.2) acquired the ability to spread rapidly after long-term culture.

As the characteristics of the MA/JFH-1 virus changed in long-term culture, we analyzed the possible mutations in the viral genome from the supernatant at each peak in core protein levels (Table 1, days at peak core levels). Nine- to 12-nucleotide mutations were found in the viral genome from each supernatant, and the detected mutations were distributed along the entire genome. Among these mutations, a common nonsynonymous mutation was found in the core region (Arg to Gly at amino acid [aa]167, R167G).

In order to test the effects of R167G on virus production, an R167G substitution was introduced into MA/JFH-1.2 as MA/JFH-1.2 replicated and produced infectious virus more efficiently than MA/JFH-1.1. HCV core protein levels in cells and medium of MA/JFH-1.2 with R167G (MA/JFH-1.2/R167G) were higher than with MA/JFH-1.2 ($P < 0.05$) (Fig. 3A and B). HCV RNA levels in the medium of MA/JFH-1.2/R167G RNA-transfected cells were also higher than with MA/JFH-1.2 ($P < 0.05$) (Fig. 3C). Infectious virus production was also increased by the R167G mutation ($P < 0.05$) (Fig. 3D) and was 8.7-fold higher than that of JFH-1 RNA-transfected cells on day 3 ($P < 0.05$) (Fig. 3D).

We then tested whether R167G was responsible for the rapid spread observed in culture supernatant after long-term culture by monitoring virus spread after infection of naïve Huh7.5.1 with culture medium taken 3 days after RNA transfection of MA/JFH-1.2 and MA/JFH-1.2/R167G at an MOI of 0.005. Core protein levels in medium from MA/JFH-1.2/R167G-infected cells increased with the same kinetics as levels of JFH-1 (Fig. 3E), and the population of core protein-positive cells was almost the same as with JFH-1-infected cells (Fig. 3F), indicating that MA/JFH-1.2/R167G virus spread as rapidly as JFH-1 virus. In contrast, we observed no infectious foci in the MA/JFH-1.2 virus-inoculated cells (Fig. 3F). These data suggest that the R167G mutation in the core region was a cell culture-adaptive mutation and that it enhanced infectious MA/JFH-1.2 virus production.

In order to determine whether R167G enhances RNA replication or other steps in the viral life cycle, we performed a single-cycle virus production assay (11) using Huh7-25 cells, a HuH-7-derived cell line lacking CD81 expression on the cell surface (1).

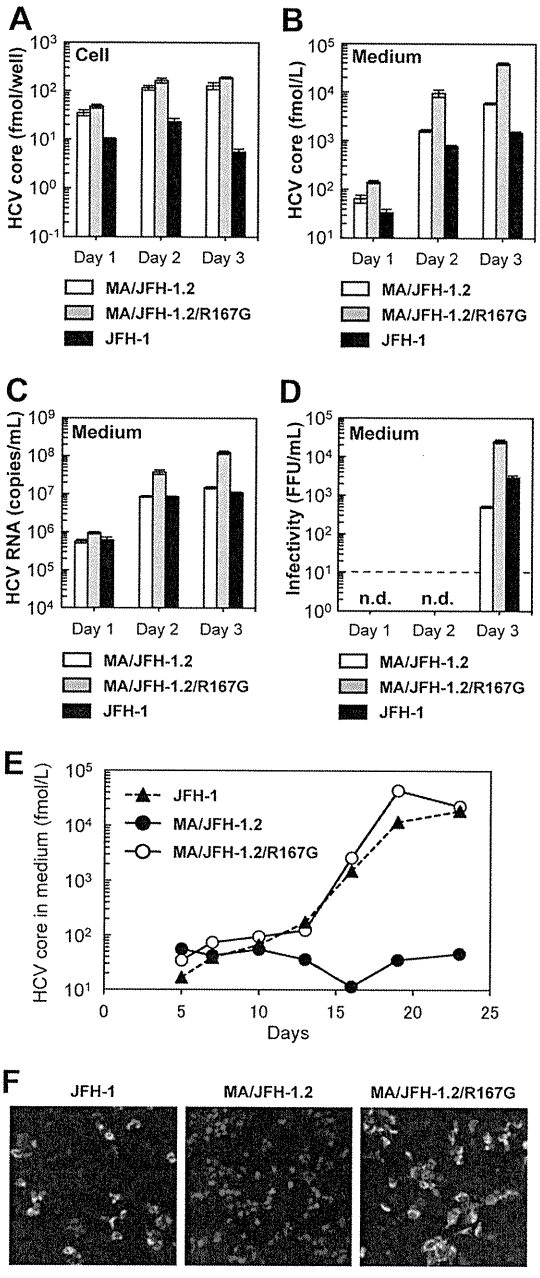


FIG 3 Effects of R167G on replication and virus production of MA/JFH-1.2 in Huh7.5.1 cells. Ten micrograms of HCV RNA was transfected into Huh7.5.1 cells, and cells and medium were harvested on days 1, 2, and 3. HCV core protein levels in the cells (A) and culture medium (B) and HCV RNA levels in the medium (C) and the infectivity of culture medium (D) from HCV RNA-transfected Huh7.5.1 cells are shown. n.d., not determined. Dashed line indicates the detection limit. Assays were performed three times independently, and data are presented as means ± standard deviation. (E) HCV core protein levels in culture medium from cells infected with medium at 3 days posttransfection at an MOI of 0.005. (F) Immunostained cells at 19 days postinfection. Infected cells were visualized with anti-core antibody (green), and nuclei were visualized with DAPI (blue).

This cell line can support replication and infectious virus production upon transfection of HCV genomic RNA but cannot be reinfected by progeny virus, thereby allowing observation of a single cycle of infectious virus production without the confounding ef-

fects of reinfection. R167G did not affect HCV core protein levels in the chimeric RNA-transfected Huh7-25 cells (Fig. 4A), demonstrating that R167G did not enhance RNA replication. Nevertheless, R167G increased HCV core protein levels in the medium ($P < 0.05$ on days 2 and 3) and infectivity (Fig. 4B and C). These results suggest that R167G did not affect RNA replication but affected other steps such as virus assembly and/or virus secretion.

Virus particle assembly efficiency was then assessed by determining intracellular-specific infectivity from infectivity and RNA titer in the cells, as reported previously (11). As shown in Fig. 4G, R167G enhanced intracellular-specific infectivity of MA/JFH-1.2 virus 10.2-fold. Virus secretion efficiency was also calculated from the amount of intracellular and extracellular infectious virus, but R167G had no effect (Fig. 4G).

To confirm the effects of Arg167 in other HCV strains, we tested its effects on JFH-1. As aa 167 of JFH-1 is Gly, we replaced it with Arg (G167R). HCV core protein levels in the cells were not affected by G167R (Fig. 4D), and no effects on RNA replication were confirmed. HCV core protein levels in the medium and infectivity decreased after G167R mutation (Fig. 4E and F). As the G167R mutation decreased intracellular infectious virus production of JFH-1 to undetectable levels, we were unable to determine the intracellular-specific infectivity and virus secretion efficiency of JFH-1 G167R (Fig. 4G). These results indicate that Gly is favored over Arg at core position 167 for infectious virus assembly in multiple HCV strains.

**MA harboring the R167G mutation, 5′ UTR, and N3H (NS3 helicase) and N5BX (NS5B to 3′ X) regions of JFH-1 replicated and produced infectious chimeric virus.** In order to establish a genotype 2b cell culture system with the MA strain with minimal regions of JFH-1, we attempted to reduce JFH-1 content in MA/JFH-1.2. We previously reported that replacement of the N3H and N5BX regions of JFH-1 allowed efficient replication of the J6CF strain, which normally cannot replicate in cells (21). Thus, we tested whether the N3H and N5BX regions of JFH-1 could also support MA RNA replication.

We prepared two chimeric MA constructs harboring the 5′ UTR and N3H and N5BX regions of JFH-1, MA/N3H+N5BX-JFH1 (Fig. 5A) and MA/N3H+N5BX-JFH1/R167G. After *in vitro* transcribed RNA was transfected into Huh7.5.1 cells, intracellular core protein levels of MA/N3H+N5BX-JFH1 and MA/N3H+N5BX-JFH1/R167G RNA-transfected cells increased in a time-dependent manner and reached almost the same levels as with MA/JFH-1.2 RNA-transfected cells on day 5 (Fig. 5B). Extracellular core protein and HCV RNA levels of MA/N3H+N5BX-JFH1 and MA/N3H+N5BX-JFH1/R167G RNA-transfected cells also increased in a time-dependent manner (Fig. 5C and D). However, they were more than 10 times lower than with MA/JFH-1.2 RNA-transfected cells although intracellular core levels were comparable on day 5 (Fig. 5B to D).

We then tested whether the medium from MA/N3H+N5BX-JFH1 and MA/N3H+N5BX-JFH1/R167G RNA-transfected cells was infectious. Infectivity of the medium from MA/N3H+N5BX-JFH1 RNA-transfected cells was below the detection limit, and that of MA/N3H+N5BX-JFH1/R167G RNA-transfected cells on day 5 was very low ($3.3 \times 10^1 \pm 2.1 \times 10^1$ FFU/ml) (Fig. 5E). To confirm infectivity, the culture media were concentrated, and their infectivity was determined. Infected foci were observed after infection with concentrated medium in MA/N3H+N5BX-JFH1/R167G RNA-transfected cells (Fig. 5F), and infectivity was found

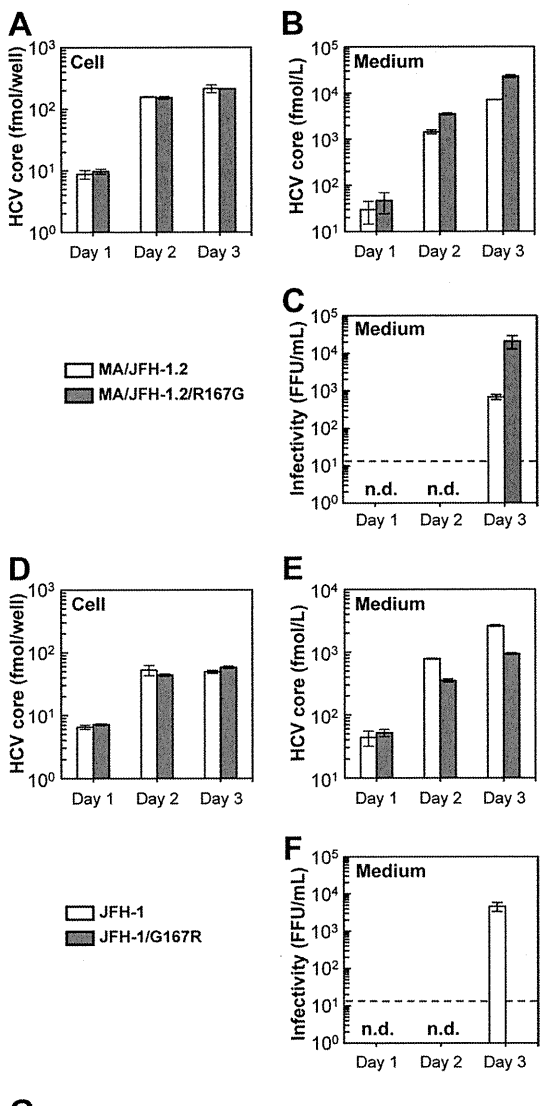


G

| Construct | Intracellular Specific Infectivity (FFU/ x10⁶ HCV RNA copies) | Infectious Virus Secretion (Extra/Intra) |
|---|---|---|
| MA/JFH-1.2 | 1.68 ± 0.404 | 20.2 ± 4.26 |
| MA/JFH-1.2/R167G | 17.1 ± 4.38 | 14.1 ± 1.65 |
| JFH-1 | 1.78 ± 0.364 | 63.3 ± 6.44 |
| JFH-1/G167R | NA | NA |

FIG 4 Effects of R167G on replication and virus production of MA/JFH-1.2 and JFH-1 in Huh7-25 cells. Ten micrograms of HCV RNA was transfected into Huh7-25 cells, and cells and medium were harvested on days 1, 2, and 3. HCV core protein levels in cells (A and D) and in medium (B and E) were measured, and infectivity of medium (C and F) was determined. n.d., not determined. Dashed line indicates the detection limit. (G) Intracellular specific infectivity and virus secretion efficiency of chimeric HCV RNA-transfected cells. Intracellular and extracellular infectivity of day 3 samples was determined, and specific infectivity and virus secretion rate were calculated. Assays were performed three times independently, and data are presented as means ± standard deviation. NA, not available.

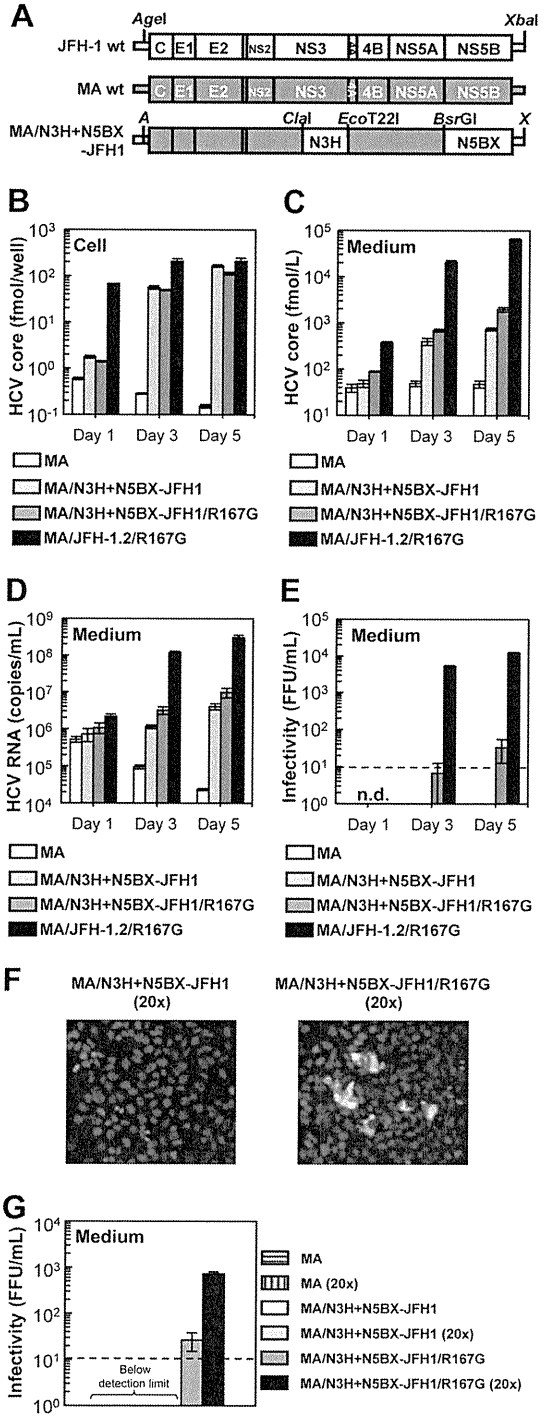


FIG 5 Replication and virus production of MA/N3H+N5BX-JFH1/R167G in Huh7.5.1 cells. (A) Schematic structures of JFH-1, MA, and MA/N3H+N5BX-JFH1. The junction of JFH-1 and MA in the 5′ UTR is an AgeI site; the junctions of MA and JFH-1 in the NS3 regions are ClaI and EcoT22I sites, and the junction in the NS5B region is a BsrGI site. A, AgeI; X, XbaI. (B to G) Chimeric HCV RNA replication in Huh7.5.1 cells. Ten micrograms of HCV RNA was transfected into Huh7.5.1 cells, and cells and medium were harvested on days 1, 3, and 5. HCV core protein levels in cells (B) and in medium (C) and HCV RNA levels in medium (D) were measured, and infectivity of medium (E) was determined. Assays were performed three times independently, and data are presented as means ± standard deviation. n.d., not determined. Dashed line indicates the detection limit. (F) Immunostained cells. Huh7.5.1 cells were infected with concentrated medium from RNA-transfected cells on day 5. Infected cells were visualized with anti-core antibody (green), and nuclei were visualized with DAPI (blue). (G) Infectivity of concentrated culture medium from HCV RNA-transfected cells. Culture medium was concentrated by 20 times. Infectivities of original and concentrated culture media were determined. Dashed line indicates detection thelimit.

to be $7.27 \times 10^2 \pm 7.57 \times 10^1$ FFU/ml (Fig. 5G). No infected foci were observed after infection of MA/N3H+N5BX-JFH1 RNA-transfected cells, even when medium was concentrated (Fig. 5F), although intracellular and extracellular core protein levels were comparable to those with MA/N3H+N5BX-JFH1/R167G RNA-transfected cells (Fig. 5B and C). These results indicate that replacement of the 5′ UTR and N3H and N5BX regions in JFH-1 were necessary to rescue autonomous replication in the replication-incompetent MA strain and for secretion of infectious chimeric virus. However, the secretion and infection efficiencies of the virus were low.

**Cell culture-adaptive mutations enhanced infectious virus production of MA/N3H+N5BX-JFH1/R167G.** Because MA/N3H+N5BX-JFH1/R167G replicated efficiently but produced very small amounts of infectious virus, we performed a long-term culture of the RNA-transfected cells in order to induce cell culture-adaptive mutations that could enhance infectious virus production. We prepared RNA-transfected cells using two constructs, MA/N3H+N5BX-JFH1 and MA/N3H+N5BX-JFH1/R167G; both of these replicated efficiently, and MA/N3H+N5BX-JFH1/R167G produced infectious virus at low levels while MA/N3H+N5BX-JFH1 did not. Immediately after transfection, the HCV core protein levels in the medium of each RNA-transfected cell culture peaked at $3.0 \times 10^3$ fmol/liter and declined thereafter. However, the core protein level in the medium with MA/N3H+N5BX-JFH1/R167G RNA-transfected cells continued to increase and reached a peak of $2.7 \times 10^5$ fmol/liter 54 days after transfection, at which point most cells were core protein positive (Fig. 6B). The core protein level in the medium with MA/N3H+N5BX-JFH1 RNA-transfected cells did not increase and core-positive cells were scarce on day 54 (Fig. 6B). We analyzed the viral genome in the culture supernatants from day 54 for possible mutations and identified four nonsynonymous mutations in the MA/N3H+N5BX-JFH1/R167G genome: L814S (NS2), R1012G, (NS2), T1106A (NS3), and V1951A (NS4B). In order to test whether these amino acid substitutions enhance infectious virus production, L814S, R1012G, T1106A, and V1951A were introduced into MA/N3H+N5BX-JFH1/R167G, and the product was designated MA/N3H+N5BX-JFH1/5am (where am indicates adaptive mutation). On day 1, although HCV core protein levels in the MA/N3H+N5BX-JFH1/5am RNA-transfected cells were higher than those of MA/N3H+N5BX-JFH1/R167G RNA-transfected cells, they were still lower than those of MA/JFH-1.2/R167G RNA-transfected cells; however, on days 3 and 5, they reached a level comparable to that of MA/JFH-1.2/R167G RNA-transfected cells (Fig. 6C). HCV core protein and HCV RNA levels in the medium of MA/N3H+N5BX-JFH1/5am RNA-transfected cells were higher than those of MA/JFH-1.2/R167G RNA-transfected cells ($P < 0.05$, Fig. 6D and 6E, respectively). MA/N3H+N5BX-JFH1/5am, containing the four additional adaptive mutations, produced infectious virus at the same level as MA/JFH-1.2/R167G on day 5 (Fig. 6F). These results indicate that the

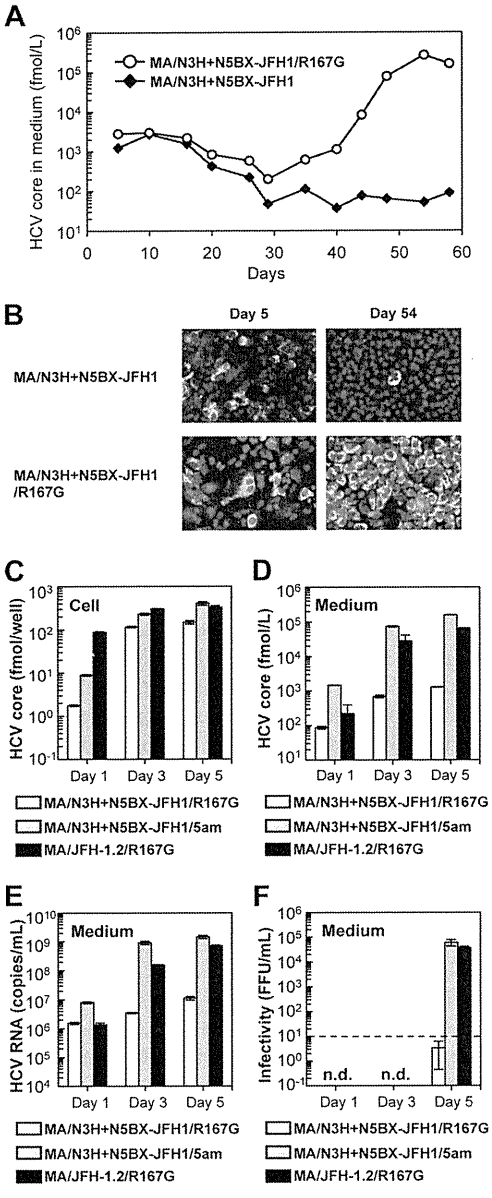


FIG 6 Cell culture-adaptive mutations enhanced infectious virus production of MA/N3H+N5BX-JFH1/R167G. (A) Long-term culture of MA/N3H+N5BX-JFH1 and MA/N3H+N5BX-JFH1/R167G RNA-transfected cells. Ten micrograms of HCV RNA was transfected into Huh7.5.1 cells, and cells were passaged every 2 to 5 days, depending on cell status. Culture medium was collected after every passage, and HCV core protein levels were measured. HCV core protein levels in culture medium from MA/N3H+N5BX-JFH1 and MA/N3H+N5BX-JFH1/R167G RNA-transfected cells are presented. (B) Immunostained cells on days 5 and 54 after transfection. Infected cells were visualized with anti-core antibody (green), and nuclei were visualized with DAPI (blue). (C to F) Effect of four additional cell culture-adaptive mutations on virus production. Ten micrograms of HCV RNA was transfected into Huh7.5.1 cells, and cells and medium were harvested on days 1, 3, and 5. HCV core levels in cells (C) and in medium (D) and HCV RNA levels in medium (E) were measured, and infectivity of medium (F) was determined. Assays were performed three times independently, and data are presented as means ± standard deviation. n.d., not determined. Dashed line indicates the detection limit.

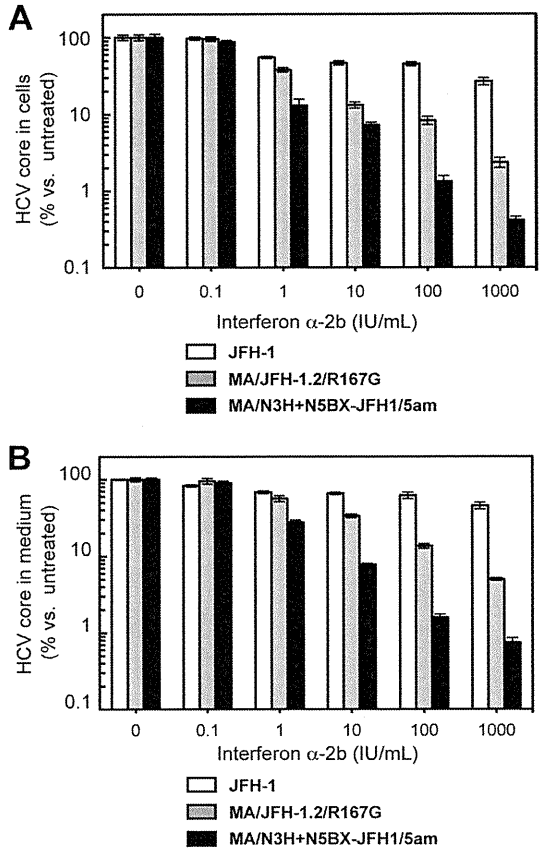


FIG 7 Comparisons of interferon sensitivity between JFH-1, MA/JFH-1.2/R167G and MA/N3H+N5BX-JFH1/5am. Two micrograms of HCV RNA was transfected into Huh7.5.1 cells, and interferon was added at the indicated concentrations at 4 h after transfection. HCV core protein levels in cells (A) and in medium (B) on day 3 were measured, and data are expressed as percent versus untreated cells (0 IU/ml). Assays were performed three times independently, and data are presented as means ± standard deviation.

four additional adaptive mutations enhance infectious virus production and that MA/N3H+N5BX-JFH1/5am RNA-transfected cells replicate and produce infectious virus as efficiently as MA/JFH-1.2/R167G RNA-transfected cells.

**Comparison of interferon sensitivity between JFH-1, MA/JFH-1.2/R167G, and MA/N3H+N5BX-JFH1/R167G.** Using the newly established genotype 2b infectious chimeric virus, we compared interferon sensitivity between the JFH-1, MA/JFH-1.2/R167G, and MA/N3H+N5BX-JFH1/5am viruses. JFH-1 or MA chimeric viral RNA-transfected Huh7.5.1 cells were treated with 0.1, 1, 10, 100, or 1,000 IU/ml interferon α-2b, and HCV core protein levels in the cells and in culture media were compared. Interferon decreased HCV core protein levels in the JFH-1 RNA-transfected cells and in the medium in a dose-dependent manner, and production was inhibited to 26.8% ± 3.0% and 45.6% ± 4.7%, respectively, of control levels (Fig. 7A and B, respectively). In contrast, HCV core protein levels in cells and medium of MA/JFH-1.2/R167G and MA/N3H+N5BX-JFH1/5am RNA-transfected cells decreased more pronouncedly in a dose-dependent manner (Fig. 7A and B, respectively). HCV core protein levels in cells and medium from MA/N3H+N5BX-JFH1/5am RNA-transfected cells were lower than those from MA/JFH-1.2/

R167G RNA-transfected cells (Fig. 7A and B, respectively) ($P < 0.05$ at 1, 10, 100, and 1,000 IU/ml), indicating that the MA/N3H+N5BX-JFH1/5am virus was more sensitive to interferon than the MA/JFH1.2/R167G virus, which contained more regions from JFH-1.

## DISCUSSION

In this study, we developed a novel infectious HCV production system using a genotype 2b chimeric virus. To improve infectious virus production, we introduced two modifications into the chimeric genome.

First, we replaced the 5′ UTR from MA with that of JFH-1. Similarly to J6/JFH-1, replacement of the 5′ UTR increased core protein accumulation in both the cells and medium when these RNAs were transfected into Huh7.5.1 cells (Fig. 1). The same trend was observed when these RNAs were transfected into Huh7-25 cells (data not shown), indicating that the 5′ UTR of JFH-1 enhanced RNA replication. There are two genetic variations in J6CF and seven in MA in the region we replaced (nt 1 to 154 for J6CF and nt 1 to 155 for MA), and some of these mutations may affect RNA replication by changing the RNA secondary structure, RNA-RNA interactions, or binding of host or viral proteins.

Second, we introduced a cell culture-adaptive mutation (R167G) in the core region. This mutation was induced by long-term culture of MA/JFH-1 RNA-transfected cells (Fig. 2). MA/JFH-1 chimeric RNA (MA/JFH-1.1 and MA/JFH-1.2) replicated when synthesized RNA was transfected into the cells. However, infectious virus production was low, and virus infection did not spread over the short term. In early stages of long-term culture, the number of core protein-positive cells gradually decreased, and core protein-positive cells were scarcely detectable. Subsequently, the population of core protein-positive cells increased, reaching almost 100%. At this time point, we identified a common mutation in the core region (R167G) of the viral genome as a cell culture-adaptive mutation and found that it enhanced infectious virus production (Fig. 3). Several nonsynonymous mutations other than R167G were identified in the viral genome from each supernatant, and these mutations may enhance infectious virus production. However, there was a discrepancy between RNA levels and the infectivity of the culture media of MA/JFH-1.2 and MA/JFH-1.2/R167G RNA-transfected cells (Fig. 3C and D). The MA/JFH-1.2/R167G mutant had a 2-log increase in viral infectivity compared to that of MA/JFH-1.2 but only a 1-log increase in secreted RNA. The replication efficiency of MA/JFH-1.2 RNA-transfected cells was comparable to that of MA/JFH-1.2/R167G RNA-transfected cells, but the efficiency of infectious virus assembly within the cells was low, indicating that mainly noninfectious virus may be produced.

Infection of MA/JFH-1.2/R167G virus spreads rapidly, similarly to that of the JFH-1 virus, when it is inoculated into naïve Huh7.5.1 cells. On a single-cycle virus production assay, we found that the R167G mutation did not affect RNA replication or virus secretion but enhanced infectious virus assembly within the cells (Fig. 4). Efficient infectious virus assembly within the cells was mainly responsible for the rapid spread and high virus production of MA/JFH-1.2/R167G.

The amino acid at 167 (aa 167) is located in domain 2 of the core region, which is important for localization of the core protein (3, 8). Lipid droplet localization of the core protein and/or NS5A is important for infectious virus production (4, 18, 26). The interaction between the core protein and NS5A is also important for infectious virus production (16). Thus, aa 167 affects infectious virus production possibly by altering subcellular localization of the core protein or interaction between the core protein and NS5A. We examined the amino acid sequence of the core protein in 2,078 strains in the Hepatitis Virus Database (http://s2as02.genes.nig.ac.jp/) and found that aa 167 is Gly in all other strains. These data strongly suggest that Gly at aa 167 is important for the HCV life cycle. As the MA strain was cloned from the serum of a patient with chronic hepatitis C, the low virus production by this Gly at aa 167 may be important for persistent infection.

We then attempted to reduce the contents of JFH-1 from MA/JFH-1.2/R167G. We previously reported that the N3H and N5BX regions of JFH-1 were sufficient for replication of the J6CF strain (21). We also reported that this effect was observed only in genotype 2a strains (J6CF, JCH-1, and JCH-4). In this study, we tested whether the N3H and N5BX regions of JFH-1 could also support replication of a genotype 2b strain, MA. We constructed an MA chimeric virus harboring the N3H and N5BX regions of JFH-1 and combined this with the 5′ UTR of JFH-1 and the R167G mutation (MA/N3H+N5BX-JFH1/R167G). This chimeric RNA was able to replicate in the cells and produce infectious chimeric virus in culture medium although infectious virus production levels were low (Fig. 5).

We showed in this paper that the N3H and N5BX regions of JFH-1 were able to support RNA replication by both genotype 2a clones and genotype 2b clones, but the nucleotide sequence similarity between JFH-1 and MA was lower than that between JFH-1 and J6CF (77% versus 89%, respectively). Compared to MA/JFH-1.2/R167G, MA/N3H+N5BX-JFH1/R167G RNA showed the same levels of RNA replication and low levels of infectious virus production. To clarify whether there were any differences in the characteristics of the secreted virus, we performed density gradient ultracentrifugation with the MA/JFH-1.2/R167G and MA/N3H+N5BX-JFH1/R167G viruses. The distributions of the HCV core protein and infectivity showed similar profiles (data not shown).

The differences between MA/JFH-1.2/R167G and MA/N3H+N5BX-JFH1/R167G are the NS2, NS3 protease domain (N3P), and NS4A to NS5A regions. Nucleotide variation(s) other than aa 167 in these regions of the MA strain may be associated with reduced virus assembly. We identified four additional cell culture-adaptive mutations, L814S (NS2), R1012G (NS2), T1106A (NS3), and V1951A (NS4B), which resulted from long-term culture of MA/N3H+N5BX-JFH1/R167G RNA-transfected cells. Consequently, cells transfected with MA/N3H+N5BX-JFH1/5am constructed by insertion of these four adaptive mutations into MA/N3H+N5BX-JFH1/R167G replicated and produced infectious virus as efficiently as MA/JFH-1.2/R167G RNA-transfected cells (Fig. 6).

This system is able to contribute to studies into the development of antiviral strategies. It has been reported that HCV genotype 2a was more sensitive to interferon therapy than HCV genotype 2b in a clinical study (20). To assess the interferon resistance of genotype 2b, a cell culture system with multiple genotype 2b strains is necessary. The previously reported replicable genotype 2b chimeric virus harbored only structural

regions of 2b strains (6, 27). The 2b/JFH-1 chimeric virus containing the region of the core protein to NS2 from the J8 strain (genotype 2b) and the region of NS3 to 3′ X of JFH-1 was able to replicate and showed that there were no differences in interferon sensitivity among the JFH-1 chimeric viruses of other genotypes (6, 27). Another 2b/JFH-1 chimeric virus containing the regions of the core protein to NS2 (nt 342 to 2867) of a genotype 2b strain and of NS2 to 3′ UTR (nt 2868) of JFH-1 has been reported (6, 27). The authors reported that their 2b/JFH-1 chimeric virus was more sensitive to interferon than JFH-1 (6, 27). We developed the genotype 2b HCV cell culture system with another HCV genotype 2b strain (MA). We identified a virus assembly-enhancing mutation in the core region, the minimal JFH-1 regions necessary for replication, and four additional adaptive mutations that enhance infectious virus production and demonstrated that MA harboring the five adaptive mutations and the 5′ UTR and N3H and N5BX regions of JFH-1 (MA/N3H+N5BX-JFH1/5am) could replicate and produce infectious virus efficiently.

Using these novel genotype 2b chimeric viruses, we assessed interferon sensitivity. We found that MA/JFH-1.2/R167G chimeric virus and MA/N3H+N5BX-JFH1/5am virus were more sensitive to interferon than the JFH-1 virus (Fig. 7). Furthermore, we found that MA/N3H+N5BX-JFH1/5am was more sensitive to interferon than MA/JFH-1.2/R167G, indicating that the genetic variation(s) in the NS2, N3P, and NS4A to NS5A regions affect interferon sensitivity. Although genotype 2a viruses are more sensitive to interferon than genotype 2b viruses in clinical studies, JFH-1 displayed interferon resistance in our study.

These results suggest that the JFH-1 regions in the 2b/JFH-1 virus affect the interferon sensitivity of the chimeric virus. Moreover, it was reported that amino acid variations in E2, p7, NS2, and NS5A were associated with the response to peginterferon and ribavirin therapy in genotype 2b HCV infection (10). Therefore, our MA/JFH-1 chimeric virus harboring minimal regions from JFH-1 (MA/N3H+N5BX-JFH1/5am) is more suitable for assessing the characteristics of the MA strain than the MA/JFH-1 chimeric virus, which includes a nonstructural region from JFH-1 (MA/JFH-1.2/R167G). We showed here that replacement of the 5′ UTR and N3H and N5BX regions in MA with those from JFH-1 is able to convert MA into a replicable virus. Using the same strategy, numerous HCV cell culture systems with various genotype 2b strains, as well as genotype 2a strains, may be available.

In conclusion, we established a novel HCV genotype 2b cell culture system using a chimeric genome in MA harboring minimal regions from JFH-1. This cell culture system using the chimeric genotype 2b virus will be useful for characterization of genotype 2b viruses and the development of antiviral strategies.

## ACKNOWLEDGMENTS

We are grateful to Tetsuro Suzuki of Hamamatsu University School of Medicine for helpful comments and suggestions. Huh7.5.1 cells were kindly provided by Francis V. Chisari.

A.M. is partially supported by the Japan Health Sciences Foundation and Viral Hepatitis Research Foundation of Japan. This work was partially supported by Grants-in-Aid for Scientific Research from the Japan Society for the Promotion of Science, from the Ministry of Health, Labor and Welfare of Japan, from the Ministry of Education, Culture, Sports, Science and Technology, from the National Institute of Biomedical Innovation, and by Research on Health Sciences Focusing on Drug Innovation from the Japan Health Sciences Foundation.

## REFERENCES

1. **Akazawa D, et al.** 2007. CD81 expression is important for the permissiveness of Huh7 cell clones for heterogeneous hepatitis C virus infection. J. Virol. **81**:5036–5045.
2. **Bartenschlager R, Lohmann V.** 2000. Replication of hepatitis C virus. J. Gen. Virol. **81**:1631–1648.
3. **Boulant S, et al.** 2006. Structural determinants that target the hepatitis C virus core protein to lipid droplets. J. Biol. Chem. **281**:22236–22247.
4. **Boulant S, Targett-Adams P, McLauchlan J.** 2007. Disrupting the association of hepatitis C virus core protein with lipid droplets correlates with a loss in production of infectious virus. J. Gen. Virol. **88**:2204–2213.
5. **Choo QL, et al.** 1989. Isolation of a cDNA clone derived from a blood-borne non-A, non-B viral hepatitis genome. Science **244**:359–362.
6. **Gottwein JM, et al.** 2009. Development and characterization of hepatitis C virus genotype 1–7 cell culture systems: role of CD81 and scavenger receptor class B type I and effect of antiviral drugs. Hepatology **49**:364–377.
7. **Griffin S, et al.** 2008. Genotype-dependent sensitivity of hepatitis C virus to inhibitors of the p7 ion channel. Hepatology **48**:1779–1790.
8. **Hope RG, McLauchlan J.** 2000. Sequence motifs required for lipid droplet association and protein stability are unique to the hepatitis C virus core protein. J. Gen. Virol. **81**:1913–1925.
9. **Jensen TB, et al.** 2008. Highly efficient JFH1-based cell-culture system for hepatitis C virus genotype 5a: failure of homologous neutralizing-antibody treatment to control infection. J. Infect. Dis. **198**:1756–1765.
10. **Kadokura M, et al.** 2011. Analysis of the complete open reading frame of genotype 2b hepatitis C virus in association with the response to peginterferon and ribavirin therapy. PLoS One **6**:e24514.
11. **Kato T, et al.** 2008. Hepatitis C virus JFH-1 strain infection in chimpanzees is associated with low pathogenicity and emergence of an adaptive mutation. Hepatology **48**:732–740.
12. **Kato T, et al.** 2006. Cell culture and infection system for hepatitis C virus. Nat. Protoc. **1**:2334–2339.
13. **Kiyosawa K, et al.** 1990. Interrelationship of blood transfusion, non-A, non-B hepatitis and hepatocellular carcinoma: analysis by detection of antibody to hepatitis C virus. Hepatology **12**:671–675.
14. **Lindenbach BD, et al.** 2005. Complete replication of hepatitis C virus in cell culture. Science **309**:623–626.
15. **Lohmann V, et al.** 1999. Replication of subgenomic hepatitis C virus RNAs in a hepatoma cell line. Science **285**:110–113.
16. **Masaki T, et al.** 2008. Interaction of hepatitis C virus nonstructural protein 5A with core protein is critical for the production of infectious virus particles. J. Virol. **82**:7964–7976.
17. **Miyamoto M, Kato T, Date T, Mizokami M, Wakita T.** 2006. Comparison between subgenomic replicons of hepatitis C virus genotypes 2a (JFH-1) and 1b (Con1 NK5.1). Intervirology **49**:37–43.
18. **Miyanari Y, et al.** 2007. The lipid droplet is an important organelle for hepatitis C virus production. Nat. Cell Biol. **9**:1089–1097.
19. **Murakami K, Abe M, Kageyama T, Kamoshita N, Nomoto A.** 2001. Down-regulation of translation driven by hepatitis C virus internal ribosomal entry site by the 3′ untranslated region of RNA. Arch. Virol. **146**:729–741.
20. **Murakami T, et al.** 1999. Mutations in nonstructural protein 5A gene and response to interferon in hepatitis C virus genotype 2 infection. Hepatology **30**:1045–1053.
21. **Murayama A, et al.** 2007. The NS3 helicase and NS5B-to-3′X regions are important for efficient hepatitis C virus strain JFH-1 replication in Huh7 cells. J. Virol. **81**:8030–8040.
22. **Murayama A, et al.** 2010. RNA polymerase activity and specific RNA structure are required for efficient HCV replication in cultured cells. PLoS Pathog. **6**:e1000885.
23. **Pietschmann T, et al.** 2006. Construction and characterization of infectious intragenotypic and intergenotypic hepatitis C virus chimeras. Proc. Natl. Acad. Sci. U. S. A. **103**:7408–7413.
24. **Pietschmann T, et al.** 2009. Production of infectious genotype 1b virus particles in cell culture and impairment by replication enhancing mutations. PLoS Pathog. **5**:e1000475.
25. **Scheel TK, et al.** 2008. Development of JFH1-based cell culture systems

for hepatitis C virus genotype 4a and evidence for cross-genotype neutralization. Proc. Natl. Acad. Sci. U. S. A. **105**:997–1002.
26. **Shavinskaya A, Boulant S, Penin F, McLauchlan J, Bartenschlager R.** 2007. The lipid droplet binding domain of hepatitis C virus core protein is a major determinant for efficient virus assembly. J. Biol. Chem. **282**: 37158–37169.
27. **Suda G, et al.** 2010. IL-6-mediated intersubgenotypic variation of interferon sensitivity in hepatitis C virus genotype 2a/2b chimeric clones. Virology **407**:80–90.
28. **Takeuchi T, et al.** 1999. Real-time detection system for quantification of hepatitis C virus genome. Gastroenterology **116**:636–642.
29. **Wakita T, et al.** 2005. Production of infectious hepatitis C virus in tissue culture from a cloned viral genome. Nat. Med. **11**:791–796.
30. **Yi M, Ma Y, Yates J, Lemon SM.** 2007. Compensatory mutations in E1, p7, NS2, and NS3 enhance yields of cell culture-infectious intergenotypic chimeric hepatitis C virus. J. Virol. **81**:629–638.
31. **Yi M, Villanueva RA, Thomas DL, Wakita T, Lemon SM.** 2006. Production of infectious genotype 1a hepatitis C virus (Hutchinson strain) in cultured human hepatoma cells. Proc. Natl. Acad. Sci. U. S. A. **103**:2310–2315.
32. **Zhong J, et al.** 2005. Robust hepatitis C virus infection in vitro. Proc. Natl. Acad. Sci. U. S. A. **102**:9294–9299.

Research Article

EASL EUROPEAN ASSOCIATION FOR THE STUDY OF THE LIVER | JOURNAL OF HEPATOLOGY

# Altered composition of fatty acids exacerbates hepatotumorigenesis during activation of the phosphatidylinositol 3-kinase pathway

Yotaro Kudo[1], Yasuo Tanaka[1], Keisuke Tateishi[1,*], Keisuke Yamamoto[1], Shinzo Yamamoto[1], Dai Mohri[1], Yoshihiro Isomura[1], Motoko Seto[1], Hayato Nakagawa[1], Yoshinari Asaoka[1], Motohisa Tada[2], Miki Ohta[1], Hideaki Ijichi[1], Yoshihiro Hirata[1], Motoyuki Otsuka[1], Tsuneo Ikenoue[1], Shin Maeda[3], Shuichiro Shiina[1], Haruhiko Yoshida[1], Osamu Nakajima[4], Fumihiko Kanai[2], Masao Omata[5], Kazuhiko Koike[1]

[1]*Department of Gastroenterology, Graduate School of Medicine, The University of Tokyo, 7-3-1 Hongo, Bunkyo-ku, Tokyo 113-8655, Japan;* [2]*Department of Medicine and Clinical Oncology, Graduate School of Medicine, Chiba University, 1-8-1 Inohana, Chuo-ku, Chiba-shi, Chiba 260-8670, Japan;* [3]*Department of Gas troenterology, Yokohama City University, Graduate School of Medicine, 3-9 Fuku-ura, Kanazawa-ku, Yokohama 236-0004, Japan;* [4]*Research Laboratory for Molecular Genetics, Yamagata University, Yamagata 990-9585, Japan;* [5]*Yamanashi Prefectural Central Hospital, 1-1-1 Fujimi, Kofu-shi, Yamanashi 400-8506, Japan*

**Background & Aims**: Some clinical findings have suggested that systemic metabolic disorders accelerate *in vivo* tumor progression. Deregulation of the phosphatidylinositol 3-kinase (PI3K)/Akt pathway is implicated in both metabolic dysfunction and carcinogenesis in humans; however, it remains unknown whether the altered metabolic status caused by abnormal activation of the pathway is linked to the protumorigenic effect.

**Methods**: We established hepatocyte-specific *Pik3ca* transgenic (Tg) mice harboring N1068fs*4 mutation.

**Results**: The Tg mice exhibited hepatic steatosis and tumor development. PPARγ-dependent lipogenesis was accelerated in the Tg liver, and the abnormal profile of accumulated fatty acid (FA) composition was observed in the tumors of Tg livers. In addition, the Akt/mTOR pathway was highly activated in the tumors, and in turn, the expression of tumor suppressor genes including *Pten*, *Xpo4*, and *Dlc1* decreased. Interestingly, we found that the suppression of those genes and the enhanced *in vitro* colony formation were induced in the immortalized hepatocytes by the treatment with oleic acid (OA), which is one of the FAs that accumulated in tumors.

**Conclusions**: Our data suggest that the unusual FA accumulation has a possible role in promoting *in vivo* hepato-tumorigenesis under constitutive activation of the PI3K pathway. The *Pik3ca* Tg mice might help to elucidate molecular mechanisms by which metabolic dysfunction contributes to *in vivo* tumor progression.


## Introduction

Accumulating clinical evidence suggests that systemic metabolic disorders including obesity and insulin resistance can affect or even promote *in vivo* tumor progression [1–4]. Some studies have outlined the impact of fat-enriched diets in the development of hepatocellular carcinoma (HCC) [5–7]. However, the mechanistic insights regarding metabolites or cellular signaling responsible for the development of HCC in altered metabolic states remain unknown.

The phosphatidylinositol 3-kinase (PI3K)/Akt signaling pathway is involved in various cellular processes including cell metabolism, growth, and survival [8,9]. The altered expression and mutation of PI3K/Akt-related signaling components have been detected in some human cancers [10]. In particular, the *PIK3CA* gene encoding p110α, which is a catalytic subunit of PI3K, has somatic mutations in some carcinomas [11]. Additionally, a mutation in its kinase domain has been reported in HCC and gastric cancer [12]. These findings indicate that deregulated PI3K activity plays certain roles in oncogenesis in humans [11,13]. PI3K signaling is antagonized by phosphatase and tensin homolog deleted on chromosome 10 (PTEN) phosphatase [14]. The expression of PTEN is decreased or absent in approximately half of HCC patients [15], and hepatocyte-specific *Pten* knockout

Keywords: Hepatocellular carcinoma; Fatty acids; NAFLD; Tumor suppressor genes.
*Received 3 October 2010; received in revised form 25 March 2011; accepted 27 March 2011; available online 19 May 2011*
*Corresponding author. Tel.: +81 3 3815 5411x33070; fax: +81 3 3814 0021.
*E-mail address:* ktate-tky@umin.ac.jp (K. Tateishi).
*Abbreviations:* PI3K, phosphatidylinositol 3-kinase; Tg, transgenic; FA, fatty acid; OA, oleic acid; HCC, hepatocellular carcinoma; PTEN, phosphatase and tensin homolog deleted on chromosome 10; FBS, fetal bovine serum; Erk, extracellular signal-regulated kinase; WT, wild type; PA, palmitic acid; H&E, hematoxylin and eosin; NASH, non-alcoholic steatohepatitis.

mice develop steatohepatitis and HCC [16]. These findings indicate that PTEN is a tumor suppressor in the liver [17]. Although recent reports have suggested unique functions of PTEN that are independent of the PI3K-Akt axis [18–20], it is unknown whether the phenotype in *Pten*-deficient mice is due to PI3K-dependent or PI3K-independent processes.

To address the pathological consequences caused by the abnormal activation of PI3K pathway *in vivo*, we generated liver-specific *Pik3ca* transgenic (Tg) mice. In this study, we proposed that abnormal fat composition, as observed in the *Pik3ca* Tg liver, is a mechanism by which metabolic deregulation is linked to *in vivo* tumor progression.

## Materials and methods

*Generation of Pik3ca Tg mice*

The *Pik3ca* Tg mice were generated as described previously [21]. Briefly, Myc-tagged mouse *Pik3ca* cDNA (N1068fs*4) was cloned into the p2335A-1 vector (provided by Drs. Palmiter and Chisari) [22,23]. The microinjection was conducted by the Research Laboratory for Molecular Genetics, Yamagata University. Founder BDF1 mice (F0) were backcrossed with C57BL/6JJcl mice (CLEA Japan, Japan), and F5 mice were analyzed. The primers for genotyping were 5′-ATGGAACAGAAACTCATCTCT-3′ and 5′-GGGTGACACTTACGAAAAT-3′. All procedures involving animals were performed in accordance with protocols approved by the institutional committee for animal research at the University of Tokyo and complied with the Guide for the Care and Use of Laboratory Animals.

*Cell cultures, viruses, and treatment with fatty acids*

Lentiviral short hairpin RNA vectors were purchased from Open Biosystems (Huntsville, AL, USA). BNL-CL2 cells were infected with the virus according to the manufacturer's protocol and selected by puromycin. BNL-CL2 cells were incubated with either 50 μmol/L fatty acids or ethanol (mock) for 12 h in the absence of fetal bovine serum (FBS) in some experiments.

*Antibodies and primers*

The primers for quantitative RT-PCR are shown in Supplementary Table 1. Antibodies against phospho-Akt (Ser473 and Thr308), Akt, phospho-extracellular signal-regulated kinase (Erk) 1/2 (Thr202/Tyr204), Erk1/2, phospho-TSC2, phospho-S6K, TSC2, S6K, and SREBP1 were obtained from Cell Signaling Technology (Danvers, MA, USA). The anti-PTEN antibody was purchased from Neomarkers Inc. (Frement, CA, USA). The anti-TFIID antibody was purchased from Upstate Biotechnology Inc. (Lake Placid, NY, USA). For immunohistochemistry, the anti-phospho-Akt (Ser473) antibody and anti-Myc antibodies (Cell Signaling Technology) were used. The immunoblot data were quantified using Multi Gauge ver. 3.1 software (Fuji Film Corp., Tokyo, Japan).

*Triacylglycerol content, serum alanine aminotransferase (ALT) levels, and FA composition*

Triacylglycerols were extracted from the liver with chloroform–methanol (2:1, v/v), and the levels were determined by the GK-GPO method (Wako, Tokyo, Japan). Serum samples for ALT measurement were collected after a 16-h starvation (SRL, Tokyo, Japan). Fatty acids were extracted from frozen liver samples, and the composition was analyzed by gas chromatography (Kotobiken Medical Laboratories, Inc., Tokyo, Japan).

*Glucose tolerance tests*

Glucose was intraperitoneally injected into 8-week-old mice fasting for 16 h (1.5 mg of glucose/g body weight). Glucose concentration was measured using the FreeStyle FREEDOM Blood Glucose Monitoring System (Nipro, Tokyo, Japan) at 0, 15, 30, 60, 90, and 120 min after injection.

*Oxidative stress evaluation*

The measurement of hydrogen peroxide concentrations was performed by the Colorimetric Hydrogen Peroxide Kit (Assay Designs, Inc., Ann Arbor, MI, USA). Thiobarbituric acid reactive substances (TBARS) were measured by the TBARS Assay Kit (ZeptoMetrix, Buffalo, NY, USA).

*Immunohistochemistry*

Antigen retrieval on paraffin sections was performed by the acetylation method. Proteins were visualized using the standard 3,3′-diaminobenzidine protocol.

*Soft agar assay*

The lower layer of 0.5% agar in media was placed in a 35-mm dish. Cells ($2.5 \times 10^4$) were suspended in the upper layer of 0.3% agar. Colonies (>25 μm in diameter) were counted after 14 days. Oleic acid (OA) (50 μmol/L) or ethanol was added to the upper layer in some experiments.

*Statistics*

All results are indicated as means ± SE. Statistics were performed by Student's *t*-test or ANOVA followed by Fisher's PLSD host-hoc test. *p*-Values <0.05 were considered statistically significant.

## Results

*Generation of hepatocyte-specific Pik3ca Tg mice*

We established 2 independent lines of hepatocyte-specific Tg mice (*Pik3ca* Tg mice) harboring an "N1068fs*4" mutation in the kinase domain [12]. Myc-tagged mutant *Pik3ca* was designed to be expressed under the albumin promoter (Supplementary Fig. 1), and the liver-specific expression of the transgene was confirmed as shown in Fig. 1A. To assess the *in vivo* effect of the *Pik3ca* N1068fs*4 transgene, we analyzed the activity of molecules downstream of PIK3CA including Akt, TSC2, and S6K via immunoblotting. The phosphorylation of Akt, TSC2, and S6K was clearly increased both in the two lines of Tg livers, but not in the wild-type (WT) livers (Fig. 1B).

*Constitutive activation of Pik3ca leads to fat accumulation in the liver*

Both lines of *Pik3ca* Tg mice survived, and no difference in total body weight was observed between *Pik3ca* Tg and WT mice at 4 or 24 weeks of age (data not shown). The *Pik3ca* Tg2 mice exhibited better glucose tolerance than WT mice at 8 weeks (Supplementary Fig. 2). The ratio of liver weight to body weight was significantly increased in the *Pik3ca* Tg mice compared to that of WT mice (Fig. 2A). The livers of 4 week-old *Pik3ca* Tg mice appeared slightly enlarged and light-colored, and they exhibited obvious fatty changes by 24 weeks (Fig. 2B). The Tg livers contained a greater volume of triacylglycerol than WT (Fig. 2C). The results of Western blotting revealed that Tg2 mice exhibited a relatively low activation of Akt and S6K as compared to Tg1 (Fig. 1B); however, hepatic triacylglycerol levels were clearly increased in the two lines Tg mice (Fig. 2C). Indeed, even Tg2 mice demonstrated an obvious fatty change in their livers by 24 weeks (Fig. 2B and D). These findings indicated that the constitutive expression of the *Pik3ca* N1068fs*4 transgene has a potential to establish *in vivo* hepatic steatosis. In addition, we found

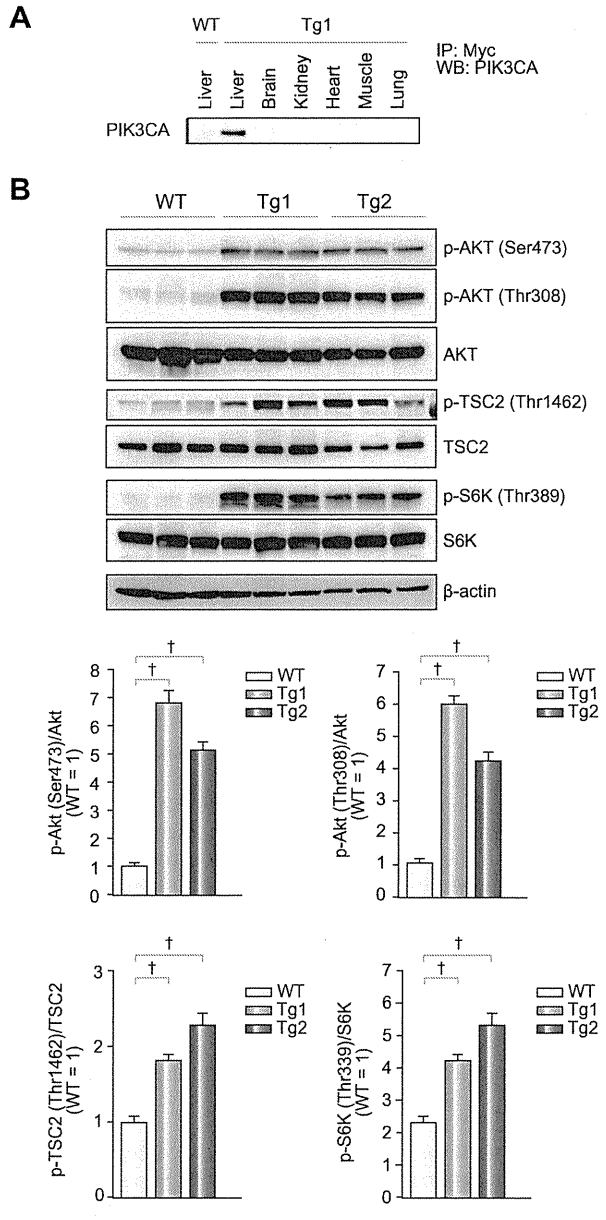


**Fig. 1. Establishment of *Pik3ca* Tg mice.** (A) Liver-specific expression of the mutant PIK3CA (N1068fs*4). (B) Immunoblots and quantification of the ratios of phosphorylated-Akt, TSC2, and S6K levels to total protein levels (†$p$ <0.05, ANOVA; post hoc test with WT).

that ALT levels in the *Pik3ca* Tg mice were higher than those of WT mice (Fig. 2E), suggesting the coexistence of liver damage. Next, we examined how the *Pik3ca* Tg liver induced unusual lipid accumulation. Because lipogenesis is mainly mediated by two major transcription factors, PPARγ and SREBP1C [24,25], we measured their expression levels and their target genes in Tg2 mice livers and observed the upregulation of PPARγ and its target aP2 but not of SREBP1C or its target FASN (Fig. 2F). Given the previous finding that activated PI3K signaling can induce steatosis through PPARγ [26], we speculated that PPARγ-dependent lipogenesis is a process responsible for hepatic steatosis in Tg mice. This was supported by the finding that the nuclear accumulation of the active form of SREBP1c protein was not increased by *Pik3ca* (N1068fs*4) expression (Supplementary Fig. 3). To emphasize this notion, we investigated whether the *in vitro* overexpression of *Pik3ca* (N1068fs*4) induced lipid accumulation and the activation of PPARγ-dependent transcription. The *in vitro* overexpression of *Pik3ca* (N1068fs*4) increased the concentration of triacylglycerol in BNL-CL2 cells, immortalized normal hepatocytes derived from a BALB/c mouse [27] (Fig. 2G), and upregulated *aP2* expression (Fig. 2H). These data indicated that the overexpression of *Pik3ca* (N1068fs*4) directly contributes to the enhanced lipogenesis, at least via activating PPARγ-dependent transcription. Given the important role of mTOR in lipogenesis through PPARγ, there is a possibility that the activation of mTOR signaling (Fig. 1B) contributes to deregulated lipogenesis through PPARγ signaling in the *Pik3ca* Tg liver [26].

### *Tumor formation without inflammation in the Pik3ca Tg mice*

Regardless of the marked fatty changes and suggested liver damage, *Pik3ca* Tg livers did not exhibit cellular infiltration or fibrotic change even at 52 weeks of age (Fig. 3A and B), which means the expression of the *Pik3ca* transgene is not sufficient for progression to steatohepatitis in the mouse liver. We found that the inflammatory cytokine IL-1α and Fas ligand were highly expressed in the *Pik3ca* Tg liver than WT (Supplementary Fig. 4). Given the previous findings that these factors can be responsible for liver damage [28,29], the abnormal upregulation of IL-1α and Fas ligand in Tg livers may explain a part of the mechanisms of liver damage, whereas the entire molecular process inducing them remains unknown. Notably, macroscopic hepatic tumors developed in 94% of Tg1 mice (30/32) and 100% of Tg2 mice (11/11) at 52 weeks of age (Fig. 3C, left). Most of the tumors were hepatocellular adenomas containing abundant lipid droplets (Fig. 3C, right). Some tumors had rough surfaces and irregular shapes with necrosis and hemorrhaging (Fig. 3D, left) and microscopically demonstrated characteristics of HCC such as enlarged and hyperchromatic nuclei and trabecular patterns (Fig. 3D, right). HCC tissues did not always exhibit lipid accumulation as shown in Fig. 3D. As the *Pik3ca* Tg mice aged, hepatic tumors became increased in number and size, whereas no WT littermates developed any tumors (Fig. 3E). These data clearly indicate that the *in vivo* constitutive expression of *Pik3ca* (N1068fs*4) leads to hepatic tumor development. To assess the functional activity of PIK3CA (N1068fs*4) for tumorigenesis, we examined the *in vitro* transforming ability using BNL-CL2 cells. Remarkably, *Pik3ca* (N1068fs*4) expression did not stimulate colony formation of BNL-CL2 cells (Supplementary Fig. 5). In addition, we analyzed the phosphorylation level of Akt by the *in vitro* overexpression of *Pik3ca* genes including wild type, H1047R, or N1068fs*4 in 293T cells. The overexpression of *Pik3ca* (H1047R) possessing *in vitro* transforming capacity [13] resulted in strong phosphorylation of Akt, as previously reported (Supplementary Fig. 6) [30]. Conversely, the overexpression of *Pik3ca* (wild type) without any transforming capacity [13] resulted in lower phosphorylation of Akt. The mutant PIK3CA (N1068fs*4) induced phosphorylation of Akt, but the level was comparable to that of wild type, and less than that of H1047R (Supplementary Fig. 6). These findings suggested that *Pik3ca* (N1068fs*4), as compared to H1047R, has less capacity for activating Akt and little

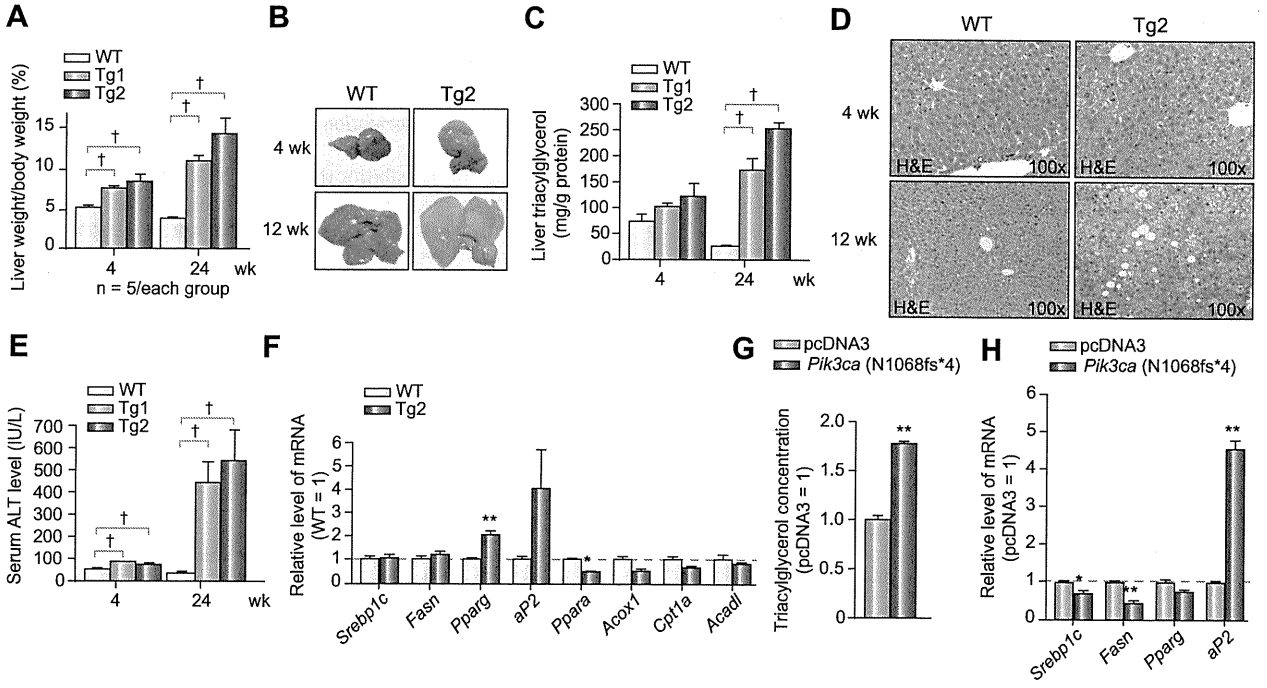


**Fig. 2. Steatosis in the *Pik3ca* Tg liver.** (A) Increased liver weight in *Pik3ca* Tg mice. (N = 5/group; †$p$ <0.05, ANOVA; post hoc test with WT). (B) Representative liver images of WT and *Pik3ca* Tg mice. (C) High concentrations of intrahepatic triacylglycerol in the Tg mice (N >5/group; †$p$ <0.05, ANOVA; post hoc test with WT). (D) H&E staining of livers from WT and *Pik3ca* Tg mice at 4 weeks (top) and 24 weeks (bottom) of age. (E) Higher serum ALT levels in the Tg mice (N = 5/group; †$p$ <0.05, ANOVA; post hoc test with WT). (F) The expression of fat metabolism genes in the 4-week-old liver (N = 3–4/group; *$p$ <0.05, **$p$ <0.01, Student's $t$-test). (G) Cellular triacylglycerol levels and (H) the expression of lipogenesis-related genes in BNL-CL2 cells stably expressing *Pik3ca* (N1068fs*4) (N = 3/group; *$p$ <0.05, **$p$ <0.01, Student's $t$-test).

oncogenic activity in itself [13] and that there might be unknown factors promoting *in vivo* tumorigenesis in the *Pik3ca* Tg liver.

*Downregulation of tumor suppressor genes in tumors derived from Pik3ca Tg livers*

To further assess the related cellular signaling for tumorigenesis in the *Pik3ca* liver, we evaluated the activation of Akt, S6K, and Erk among the WT liver, non-tumor Tg liver, and tumor tissues from 52-week-old mice (Fig. 4A). Tumor tissues exhibited significantly enhanced activation of Akt compared to the Akt activation in non-tumor background or WT livers. We observed stronger phosphorylation of Akt in the non-tumor Tg liver than in WT livers, but the difference was not statistically significant as determined by ANOVA. Furthermore, the immunohistochemistry for phospho-Akt did not demonstrate clear differences between non-tumor livers and WT tissues. In contrast, the expression of *Myc-Pik3ca* was sustained in the non-tumor liver at 52 weeks (Supplementary Fig. 7). Those findings suggest the possibility that continuous activation of Akt induced by overexpressed *Pik3ca* is important for tumor formation in the Tg livers [31], whereas it remains unknown why Akt phosphorylation was attenuated in the non-tumor liver at 52 weeks despite the sustained expression of *Pik3ca* (Fig. 4A and Supplementary Fig. 7). In addition, the phosphorylation of S6K and Erk tended to be higher in Tg livers than in WT livers (Fig. 4A), but the difference became attenuated at 52 weeks compared to that at 4 weeks (Figs. 1B and 4A and Supplementary Fig. 8). These data do not exclude the possible role of these molecules in tumorigenesis in Tg livers but at least may emphasize the importance of Akt activation. Next, we examined the expression levels of genes involved in murine hepatotumorigenesis [32–34]. We observed decreased expression of four tumor suppressor genes, *Pten*, AT-rich interactive domain 5B (*Arid5b*), exportin 4 (*Xpo4*), and deleted in liver cancer 1 (*Dlc1*), in the tumor compared to the non-tumor background of *Pik3ca* Tg livers (Fig. 4B and Supplementary Fig. 9). PTEN protein levels were downregulated (Fig. 4C). To address whether the downregulation of *Pten* contributes to the tumorigenic activity in liver cells, we established *Pten*-depleted BNL-CL2 cells (Fig. 4D). *Pten*-depleted BNL-CL2 cells generated significantly more colonies in soft agar (Fig. 4E), indicative of enhanced tumorigenicity. These findings emphasize the possibility that the decreased expression of tumor suppressor genes has a certain role in tumorigenesis in the *Pik3ca* Tg liver. Importantly, the *in vitro* overexpression of mutant *Pik3ca* (N1068fs*4) only suppressed *Arid5b* expression but did not decrease the expression of *Pten*, *Xpo4*, or *Dlc1* in BNL-CL2 cells, indicating that certain additional mechanisms repressed their expression (Supplementary Fig. 10). Although several reports suggested a relationship between oxidative stress and hepatocarcinogenesis [35], the levels of hydrogen peroxide and lipid peroxidation were comparable between Tg and WT livers (Supplementary Fig. 11).

*Tumors contain higher concentrations of OAs and palmitic acids (PAs) compared to the background tissues in the Pik3ca Tg liver*

Recent intensive research has shed light into the significance of fatty acid (FA) as a potent biological stimulator of intracellular

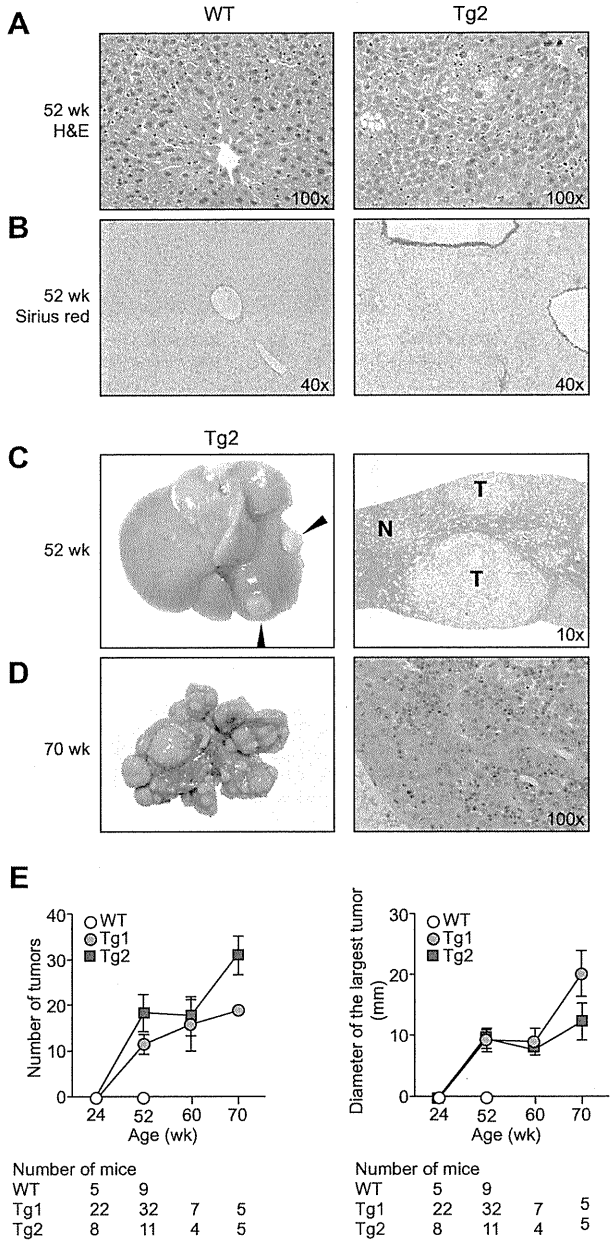


**Fig. 3. Liver tumors in the *Pik3ca* Tg mice.** (A) H&E and (B) Sirius red staining of livers at 52 weeks. (C) Macroscopic view (left) of the representative liver adenomas (arrowheads) at 52 weeks of age. H&E staining of an adenoma (T) and adjacent parenchyma (N) (right). (D) Tumors in *Pik3ca* Tg mice at 70 weeks (left). H&E staining of HCC (right). (E) The number (left) and size (right) of hepatic tumors. The number of mice examined is shown below the graphs.

signaling [36]. Interestingly, unsaturated FAs inhibit *Pten* expression via microRNA-21 in hepatoma [7,37,38], and the overexpression of a FA receptor (FFAR2) transformed the 3T3 fibroblasts [39], suggesting the possible relationship between FA and tumorigenesis. In the *Pik3ca* Tg liver, the tumor tissues contained higher concentrations of FAs than the non-tumor background tissues (Fig. 5A). The difference in total FA levels was largely due to the increase in levels of OA (C18:1n9) and PA (C16:0) in the tumors (Fig. 5B and C, Supplementary Fig. 12 and Table 2).

*OA has the potential to repress the expression of tumor suppressors and enhance colony formation in vitro*

To examine the possibility that either OA or PA downregulates the expression of tumor suppressors including *Pten*, we treated BNL-CL2 cells with OA or PA. OA, but not PA, repressed the expression of *Pten*, *Arid5b*, *Xpo4*, and *Dlc1* (Fig. 6A). Moreover, BNL-CL2 cells exposed to OA formed significantly more colonies in soft agar (Fig. 6B). These findings indicate that OA potentially enhances the in *vivo* tumorigenesis in the *Pik3ca* Tg liver. As an example, it is likely that decreased PTEN expression could enhance the Akt activation by the *Pik3ca* transgene in Tg-derived tumors (Fig. 1B).

## Discussion

Hepatocyte-specific overexpression of *Pik3ca* (N1068fs*4) leads to steatosis and hepatic tumor formation. This mutation was originally isolated in human HCC and gastric cancers [12], but its functional analysis has never been reported. The *in vitro* overexpression of this mutant clearly induced Akt activation, but the level of activation was comparable with that of *Pik3ca* wild type and lower than that of the oncogenic H1047R mutant, suggesting that the *Pik3ca* Tg mice provide a model for studying effects of PIK3CA overexpression rather than a gain-of-function of PIK3CA. Furthermore, the N1068fs*4 mutation was not sufficient for cellular transformation *in vitro*, different from *Pik3ca* H1047R [40]. Considering results from a previous report suggesting the pivotal role of Akt activation in cell transformation by *PIK3CA* mutation [13], the activation level of Akt induced by *Pik3ca* (N1068fs*4) expression should not be sufficient for the cell-transforming process. These data indicated that the development of hepatic tumors in Tg mice might not be always a direct effect of *Pik3ca* (N1068fs*4) but instead promoted by other *in vivo* protumorigenic factors.

We focused on FA as an additional protumorigenic factor contributing to *in vivo* hepato-tumorigenesis in Tg mice, based on recent research on their oncogenic capacity [39]. Previous studies reported that OA inhibits *PTEN* expression via the upregulation of microRNA-21 through an mTOR/NF-κB-dependent mechanism [37,38] and also that exposure to OA increases tumor growth in xenografts [7]. Here, we demonstrated the correlation between OA accumulation and downregulation of other tumor suppressors, whereas the entire molecular mechanism remains to be elucidated. At least, there is a possibility that, in the Tg-derived tumors, OA accumulation enhanced the Akt activation by the *Pik3ca* transgene, which phosphorylates Akt less strongly than other oncogenic mutants *in vitro* (Fig. 1B, Supplementary Figs. 6 and 13).

Lipogenesis is mainly mediated by two major transcription factors, PPARγ and SREBP1C [24,25]. Hepatocyte-specific *Pten* KO mice exhibited increased expression of both PPARγ and SREBP1c in the liver, whereas only PPARγ was highly expressed in the *Pik3ca* Tg liver [16]. Our *in vitro* data suggested that the PI3K signaling is upstream of the activation of PPARγ in hepatocytes. A recent study shows that levels of *PPARγ* as well as *SREBP1c* mRNA are higher in the livers of patients with steatosis

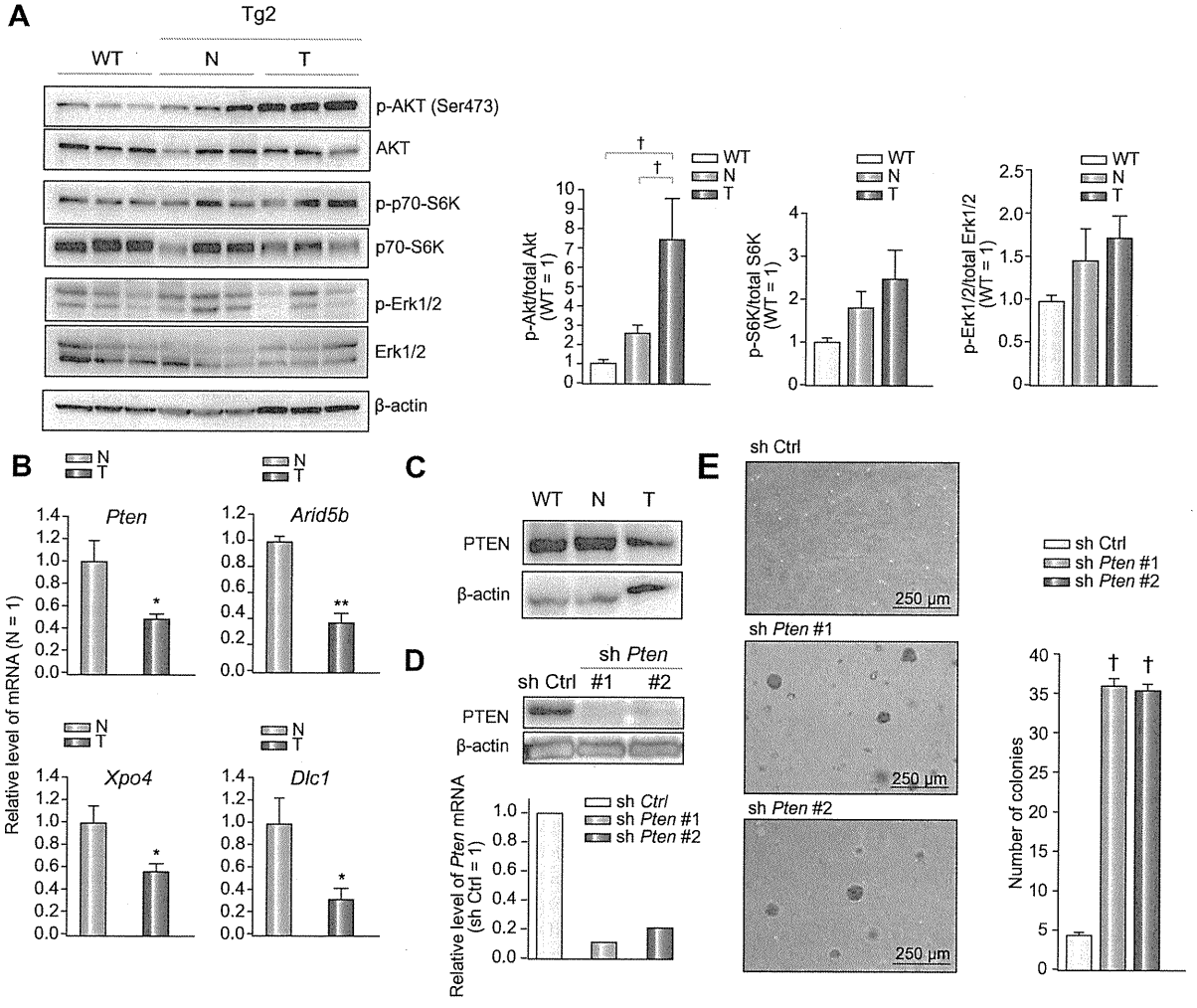


**Fig. 4. *Pten* downregulation in the *Pik3ca* Tg liver.** (A) Immunoblots and quantification of liver homogenates at 52 weeks (†$p$ <0.05, ANOVA; post hoc test with WT). (B) The decreased expression of *Pten*, *Arid5b*, *Xpo4*, and *Dlc1* mRNA in the *Pik3ca* Tg liver tumors (T) relative to their expression in background liver tissues (N) (N = 5/group; *$p$ <0.05, **$p$ <0.01, Student's $t$-test). (C) Representative images of immunoblots of liver tissues from the littermates at 52 weeks. (D) Knockdown of *Pten* in BNL-CL2 cells confirmed at the protein (top) and mRNA (bottom) levels. (E) Both lines of *Pten*-depleted BNL-CL2 cells (sh*Pten* #1 and #2) formed more colonies in soft agar (N = 3/group; † $p$ <0.05, ANOVA; post hoc test with control cells (shCtrl)).

or steatohepatitis, suggesting that the activity of PPARγ is implicated in the abnormal lipid accumulation in human livers [41] (Supplementary Fig. 13).

Unlike the hepatocyte-specific *Pten* KO mice [16], cellular infiltration and fibrosis were not observed in the *Pik3ca* Tg liver. One explanation is the possibility that *Pten* deficiency induces certain pathological mechanisms independently of PI3K-Akt activation, as previously reported for mammary tumorigenesis [18–20,42–45]. Indeed, although genetic changes in PTEN result in potent Akt phosphorylation, *in vivo* studies have suggested that they show distinct phenotypes [42]. The conditional knockout of PTEN enhanced tumorigenesis in the mammary gland [43]; however, transgenic mice expressing constitutively active Akt in the mammary gland did not show tumor formation [44]. PTEN directly associates with p53, thereby increasing its stability, protein level, and transcriptional activity [18,19]. PTEN induces apoptosis and cell cycle arrest through PI3K/Akt-independent pathways [20]. PTEN also has important roles in integrin signaling and has the ability to dephosphorylate focal adhesion kinase, reducing cell adhesion and enhancing migration [46]. These findings support an alternative mechanism of PTEN-mediated tumorigenesis independent on PI3K/Akt pathway. As a second reason for the difference from *Pten* KO mice, it is possible that PI3K catalytic beta has a distinct role with PIK3CA in the phenotype of *Pten* deficiency [47].

The discrepancy between the scarce inflammatory levels in the *Pik3ca* Tg liver and the strong increase in serum ALT levels indicative of severe liver injury is to be solved in the near future. We found that inflammatory cytokine IL-1α and Fas ligand were more highly expressed in the *Pik3ca* Tg liver than in the WT liver (Supplementary Fig. 4). Taking into account reports demonstrating that these factors can lead to liver damage [28,29], it can be suggested that their abnormal upregulation in Tg livers is in part responsible for liver damage, whereas the entire molecular process inducing them remains unknown (Supplementary Fig. 13).

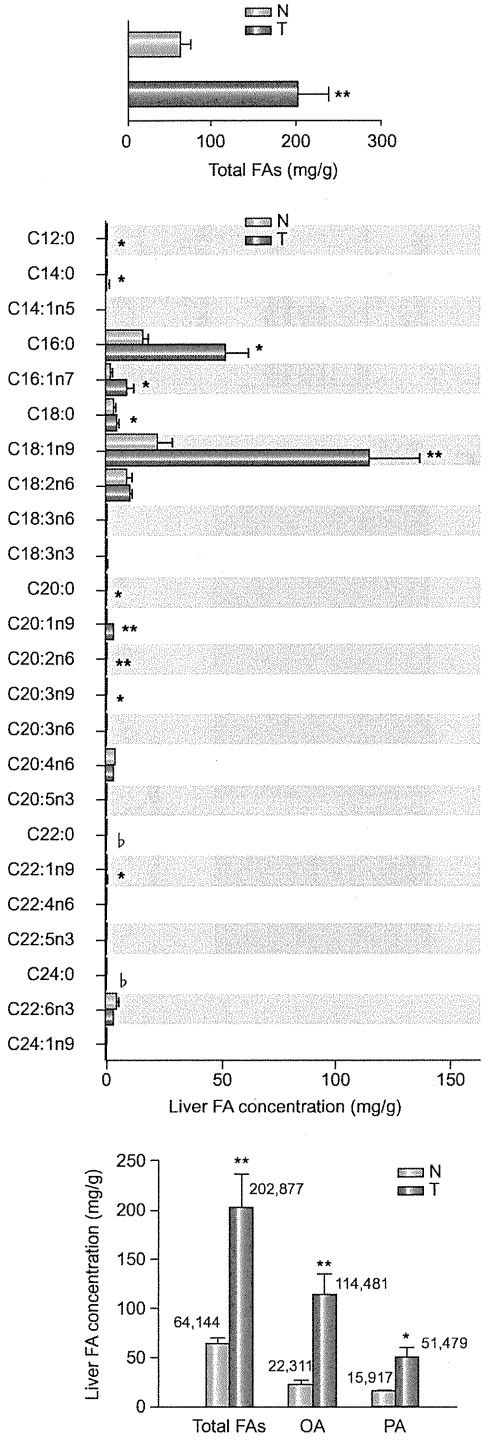


**Fig. 5. The total FA composition in the *Pik3ca* Tg liver tissues and tumors.** (A) The levels of FAs in the tumor (T) and non-tumor background tissue (N) in *Pik3ca* Tg mice at 52 weeks (N = 4/group; $^{**}p$ <0.01, Student's *t*-test). (B) FA composition in background (N) and tumor tissues (T) (N = 4/group; statistically increased FA levels in the tumors are shown with asterisks ($^{*}p$ <0.05, $^{**}p$ <0.01) and significantly decreased levels are shown with flat (μ, $p$ <0.05), Student's *t*-test). (C) The concentration of total FAs, OA, and PA in background (N) and tumor tissues (T) (N = 4/group; $^{*}p$ <0.05, $^{**}p$ <0.01, Student's *t*-test).

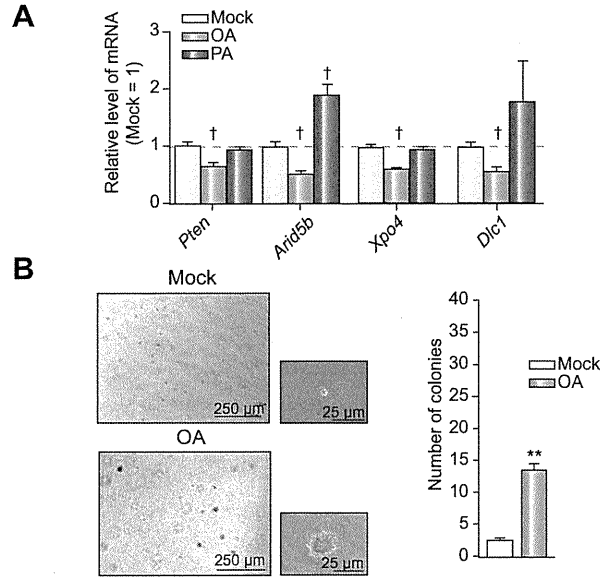


**Fig. 6. OA enhances the colony-forming activity of immortalized hepatocytes.** (A) OA but not PA decreased *Pten*, *Arid5b*, *Xpo4*, and *Dlc1* mRNA *in vitro* (N = 3/group; $^{\dagger}p$ <0.05, ANOVA; post hoc test with Mock group). (B) Colony formation assay of BNL-CL2 cells with or without 50 μmol/L OA in 10% or 0.5% FBS media (N = 3/group; $^{**}p$ <0.01, Student's *t*-test).

Mechanisms involved in the pathogenesis of non-alcoholic steatohepatitis (NASH) remain unclear, but the "two-hit theory" is widely accepted [48]. That is, in the first hit, insulin-resistance is followed by lipid accumulation in the liver, and the second hit, possibly involving inflammatory cytokines or oxidative stress, results in hepatic injury and fibrosis. It has been reported that ROS has certain roles in *in vivo* carcinogenesis [35], and the concentration of ROS is upregulated in the liver suffering NASH or NASH-derived HCC [49]. Regardless of the obvious fatty liver, our model mice have not shown impaired glucose tolerance. The concentration of ROS in the *Pik3ca* Tg mice was comparable with that of WT mice (Supplementary Fig. 11), which can be partly explained by the lower expression of fat-oxidative genes (Fig. 2F) and lack of inflammatory cell infiltration. These findings indicate that *Pik3ca* Tg mice do not always mimic the entire pathological mechanisms causing NASH, while they might be useful as a prototype to determine which pathological processes are required for the progression from the fatty liver to NASH. In addition, given the low rate of HCC development in these mice, they can be potentially useful for discovering tumor-promoting factors in hepatic steatosis. For example, although it was unlikely that ROS is involved in the initiation of hepatic tmor in the *Pik3ca* Tg liver, we can examine the pathological significance of ROS in tumor progression as well as hepatitis induction by applying the *Pik3ca* Tg liver to the condition producing high levels of ROS.

Recent clinical findings have advocated the relationship between volume of visceral fat and tumor progression [1–4]. While there is no direct molecular evidence to address the notion that abnormal body fat accumulation accelerates tumor growth, our data might provide new insights into the mechanisms of the "lipotoxicity-related" tumorigenesis. Future researches are needed to unravel how OA affects gene expression.

### Conflict of interest

The authors who have taken part in this study declared that they do not have anything to disclose regarding funding or conflict of interest with respect to this manuscript.

### Financial support

This study was supported, in part, by Health and Labor Sciences Research Grants for Research on Hepatitis from the Ministry of Health, Labor, and Welfare of Japan, by Grants-in-Aid for Scientific Research from the Ministry of Education, Culture, Sports, Science, and Technology of Japan, by The Mishima-Kaiun foundation, by the Ichiro Kanehara Foundation, by Sankyo Foundation of Life Science, by Takeda Science Foundation, by The Mochida Memorial Foundation for Medical and Pharmaceutical Research and by The Sumitomo Foundation.

### Acknowledgments

We thank Dr. Richard D. Palmiter (Howard Hughes Medical Institute and Department of Biochemistry, University of Washington, Seattle, USA) and Francis V. Chisari (Department of Molecular and Experimental Medicine, Scripps Research Institute, La Jolla, USA) for providing the plasmid. We also thank Dr. Junji Shibahara (Department of Pathology, Graduate School of Medicine, The University of Tokyo) and Kojiro Ueki (Department of Metabolic Diseases, Graduate School of Medicine, The University of Tokyo) for helpful discussions, and Mitsuko Tsubouchi for technical assistance.

### Supplementary data

Supplementary data associated with this article can be found, in the online version, at doi:10.1016/j.jhep.2011.03.025.

### References

[1] Garfinkel L. Overweight and cancer. Ann Intern Med 1985;103:1034–1036.
[2] Deslypere JP. Obesity and cancer. Metabolism 1995;44:24–27.
[3] Schapira DV, Clark RA, Wolff PA, Jarrett AR, Kumar NB, Aziz NM. Visceral obesity and breast cancer risk. Cancer 1994;74:632–639.
[4] Yamaji Y, Okamoto M, Yoshida H, Kawabe T, Wada R, Mitsushima T, et al. The effect of body weight reduction on the incidence of colorectal adenoma. Am J Gastroenterol 2008;103:2061–2067.
[5] Hill-Baskin AE, Markiewski MM, Buchner DA, Shao H, DeSantis D, Hsiao G, et al. Diet-induced hepatocellular carcinoma in genetically predisposed mice. Hum Mol Genet 2009;18:2975–2988.
[6] Park EJ, Lee JH, Yu GY, He G, Ali SR, Holzer RG, et al. Dietary and genetic obesity promote liver inflammation and tumorigenesis by enhancing IL-6 and TNF expression. Cell 2010;140:197–208.
[7] Vinciguerra M, Carrozzino F, Peyrou M, Carlone S, Montesano R, Benelli R, et al. Unsaturated fatty acids promote hepatoma proliferation and progression through downregulation of the tumor suppressor PTEN. J Hepatol 2009;50:1132–1141.
[8] Engelman JA, Luo J, Cantley LC. The evolution of phosphatidylinositol 3-kinases as regulators of growth and metabolism. Nat Rev Genet 2006;7:606–619.
[9] Bader AG, Kang S, Zhao L, Vogt PK. Oncogenic PI3K deregulates transcription and translation. Nat Rev Cancer 2005;5:921–929.
[10] Vivanco I, Sawyers CL. The phosphatidylinositol 3-kinase AKT pathway in human cancer. Nat Rev Cancer 2002;2:489–501.
[11] Samuels Y, Diaz Jr LA, Schmidt-Kittler O, Cummins JM, Delong L, Cheong I, et al. Mutant PIK3CA promotes cell growth and invasion of human cancer cells. Cancer cell 2005;7:561–573.
[12] Lee JW, Soung YH, Kim SY, Lee HW, Park WS, Nam SW, et al. PIK3CA gene is frequently mutated in breast carcinomas and hepatocellular carcinomas. Oncogene 2005;24:1477–1480.
[13] Ikenoue T, Kanai F, Hikiba Y, Obata T, Tanaka Y, Imamura J, et al. Functional analysis of PIK3CA gene mutations in human colorectal cancer. Cancer Res 2005;65:4562–4567.
[14] Myers MP, Pass I, Batty IH, Van der Kaay J, Stolarov JP, Hemmings BA, et al. The lipid phosphatase activity of PTEN is critical for its tumor suppressor function. Proc Natl Acad Sci USA 1998;95:13513–13518.
[15] Hu TH, Huang CC, Lin PR, Chang HW, Ger LP, Lin YW, et al. Expression and prognostic role of tumor suppressor gene PTEN/MMAC1/TEP1 in hepatocellular carcinoma. Cancer 2003;97:1929–1940.
[16] Horie Y, Suzuki A, Kataoka E, Sasaki T, Hamada K, Sasaki J, et al. Hepatocyte-specific Pten deficiency results in steatohepatitis and hepatocellular carcinomas. J Clin Invest 2004;113:1774–1783.
[17] Vinciguerra M, Foti M. PTEN at the crossroad of metabolic diseases and cancer in the liver. Ann Hepatol 2008;7:192–199.
[18] Freeman DJ, Li AG, Wei G, Li HH, Kertesz N, Lesche R, et al. PTEN tumor suppressor regulates p53 protein levels and activity through phosphatase-dependent and -independent mechanisms. Cancer Cell 2003;3:117–130.
[19] Li AG, Piluso LG, Cai X, Wei G, Sellers WR, Liu X. Mechanistic insights into maintenance of high p53 acetylation by PTEN. Mol Cell 2006;23:575–587.
[20] Weng L, Brown J, Eng C. PTEN induces apoptosis and cell cycle arrest through phosphoinositol-3-kinase/Akt-dependent and -independent pathways. Hum Mol Genet 2001;10:237–242.
[21] Nakajima O, Okano S, Harada H, Kusaka T, Gao X, Hosoya T, et al. Transgenic rescue of erythroid 5-aminolevulinate synthase-deficient mice results in the formation of ring sideroblasts and siderocytes. Genes Cells 2006;11:685–700.
[22] Pasquinelli C, Shoenberger JM, Chung J, Chang KM, Guidotti LG, Selby M, et al. Hepatitis C virus core and E2 protein expression in transgenic mice. Hepatology 1997;25:719–727.
[23] Pinkert CA, Ornitz DM, Brinster RL, Palmiter RD. An albumin enhancer located 10 kb upstream functions along with its promoter to direct efficient, liver-specific expression in transgenic mice. Genes Dev 1987;1:268–276.
[24] Browning JD, Horton JD. Molecular mediators of hepatic steatosis and liver injury. J Clin Invest 2004;114:147–152.
[25] Gavrilova O, Haluzik M, Matsusue K, Cutson JJ, Johnson L, Dietz KR, et al. Liver peroxisome proliferator-activated receptor gamma contributes to hepatic steatosis, triglyceride clearance, and regulation of body fat mass. J Biol Chem 2003;278:34268–34276.
[26] Laplante M, Sabatini DM. An emerging role of mTOR in lipid biosynthesis. Curr Biol 2009;19:R1046–R1052.
[27] Patek PQ, Collins JL, Cohn M. Transformed cell lines susceptible or resistant to in vivo surveillance against tumorigenesis. Nature 1978;276:510–511.
[28] Sakurai T, He G, Matsuzawa A, Yu G-Y, Maeda S, Hardiman G, et al. Hepatocyte necrosis induced by oxidative stress and IL-1α release mediate carcinogen-induced compensatory proliferation and liver tumorigenesis. Cancer Cell 2008;14:156–165.
[29] Ogasawara J, Watanabe-Fukunaga R, Adachi M, Matsuzawa A, Kasugai T, Kitamura Y, et al. Lethal effect of the anti-Fas antibody in mice. Nature 1993;364:806–809.
[30] Gymnopoulos M, Elsliger MA, Vogt PK. Rare cancer-specific mutations in PIK3CA show gain of function. Proc Natl Acad Sci USA 2007;104:5569–5574.
[31] Aoki M, Batista O, Bellacosa A, Tsichlis P, Vogt PK. The Akt kinase: molecular determinants of oncogenicity. Proc Natl Acad Sci USA 1998;95:14950–14955.
[32] Zender L, Xue W, Zuber J, Semighini CP, Krasnitz A, Ma B, et al. An oncogenomics-based in vivo RNAi screen identifies tumor suppressors in liver cancer. Cell 2008;135:852–864.
[33] Xue W, Krasnitz A, Lucito R, Sordella R, Vanaelst L, Cordon-Cardo C, et al. DLC1 is a chromosome 8p tumor suppressor whose loss promotes hepatocellular carcinoma. Genes Dev 2008;22:1439–1444.
[34] Zeng Q, Hong W. The emerging role of the hippo pathway in cell contact inhibition, organ size control, and cancer development in mammals. Cancer Cell 2008;13:188–192.
[35] Ishii H, Horie Y, Ohshima S, Anezaki Y, Kinoshita N, Dohmen T, et al. Eicosapentaenoic acid ameliorates steatohepatitis and hepatocellular carcinoma in hepatocyte-specific Pten-deficient mice. J Hepatol 2009;50:562–571.

[36] Suganami T, Tanimoto-Koyama K, Nishida J, Itoh M, Yuan X, Mizuarai S, et al. Role of the Toll-like receptor 4/NF-kappaB pathway in saturated fatty acid-induced inflammatory changes in the interaction between adipocytes and macrophages. Arterioscler Thromb Vasc Biol 2007;27:84–91.
[37] Vinciguerra M, Veyrat-Durebex C, Moukil MA, Rubbia-Brandt L, Rohner-Jeanrenaud F, Foti M. PTEN down-regulation by unsaturated fatty acids triggers hepatic steatosis via an NF-kappaBp65/mTOR-dependent mechanism. Gastroenterology 2008;134:268–280.
[38] Vinciguerra M, Sgroi A, Veyrat-Durebex C, Rubbia-Brandt L, Buhler LH, Foti M. Unsaturated fatty acids inhibit the expression of tumor suppressor phosphatase and tensin homolog (PTEN) via microRNA-21 up-regulation in hepatocytes. Hepatology 2009;49:1176–1184.
[39] Hatanaka H, Tsukui M, Takada S, Kurashina K, Choi YL, Soda M, et al. Identification of transforming activity of free fatty acid receptor 2 by retroviral expression screening. Cancer Sci 2010;101:54–59.
[40] Kang S, Bader AG, Vogt PK. Phosphatidylinositol 3-kinase mutations identified in human cancer are oncogenic. Proc Natl Acad Sci USA 2005; 102:802–807.
[41] Pettinelli P, Videla LA. Up-regulation of PPAR-γ mRNA expression in the liver of obese patients: an additional reinforcing lipogenic mechanism to SREBP-1c induction. J Clin Endocrinol Metab 2011;96:1424–1430.
[42] Blanco-Aparicio C, Renner O, Leal JF, Carnero A. PTEN, more than the AKT pathway. Carcinogenesis 2007;28:1379–1386.
[43] Li G, Robinson GW, Lesche R, Martinez-Diaz H, Jiang Z, Rozengurt N, et al. Conditional loss of PTEN leads to precocious development and neoplasia in the mammary gland. Development 2002;129:4159–4170.
[44] Ackler S, Ahmad S, Tobias C, Johnson MD, Glazer RI. Delayed mammary gland involution in MMTV-AKT1 transgenic mice. Oncogene 2002;21: 198–206.
[45] Hutchinson J, Jin J, Cardiff RD, Woodgett JR, Muller WJ. Activation of Akt (protein kinase B) in mammary epithelium provides a critical cell survival signal required for tumor progression. Mol Cell Biol 2001;21:2203–2212.
[46] Tamura M, Gu J, Matsumoto K, Aota S, Parsons R, Yamada KM. Inhibition of cell migration, spreading, and focal adhesions by tumor suppressor PTEN. Science 1998;280:1614–1617.
[47] Jia S, Liu Z, Zhang S, Liu P, Zhang L, Lee SH, et al. Essential roles of PI(3)K-p110beta in cell growth, metabolism and tumorigenesis. Nature 2008;454: 776–779.
[48] Day CP, James OF. Steatohepatitis: a tale of two "hits"? Gastroenterology 1998;114:842–845.
[49] Malaguarnera L, Madeddu R, Palio E, Arena N, Malaguarnera M. Heme oxygenase-1 levels and oxidative stress-related parameters in non-alcoholic fatty liver disease patients. J Hepatol 2005;42:585–591.

Hepatology Research

*Hepatology Research* 2011; 41: 1199–1207 doi: 10.1111/j.1872-034X.2011.00871.x

*Original Article*

# Diagnostic accuracy of α-fetoprotein and des-γ-carboxy prothrombin in screening for hepatocellular carcinoma in liver transplant candidates

Noriyo Yamashiki,[1] Yasuhiko Sugawara,[2] Sumihito Tamura,[2] Junichi Kaneko,[2] Haruhiko Yoshida,[1] Taku Aoki,[2] Kiyoshi Hasegawa,[2] Masaaki Akahane,[3] Kuni Ohtomo,[3] Masashi Fukayama,[4] Kazuhiko Koike[1] and Norihiro Kokudo[2]

[1]*Department of Gastroenterology,* [2]*The Artificial Organ and Transplantation Division, Department of Surgery,* [3]*Department of Radiology, and* [4]*Department of Pathology, Graduate School of Medicine, The University of Tokyo, Tokyo, Japan*

*Aim:* Although hepatocellular carcinoma (HCC)-specific serum tumor markers, α-fetoprotein (AFP) and des-γ-carboxy prothrombin (DCP), are used in the screening for HCC, their utility in pre-transplantation evaluation is not well established. This study aimed to evaluate the accuracy of AFP and DCP measurement for the diagnosis of HCC in liver transplant candidates.

*Methods:* A total of 315 consecutive adult patients (174 men and 141 women, mean age 52 years), who were to receive liver transplantation for end-stage liver diseases, were enrolled. The pre-transplant levels of AFP and DCP were compared with the histopathology of explanted liver.

*Results:* Hepatocellular carcinoma was present in the explanted liver of 106 recipients (median number of nodules 2, mean diameter 2.5 cm). The area under receiver operating characteristic curve for the diagnosis of HCC was 0.83 (95% confidence interval, 0.78–0.88) for AFP and 0.47 (0.41–0.54) for DCP. With the cut-off value of 100 mAU/mL, 20/106 (18.9%) patients with HCC and 54/194 (27.8%) patients without HCC were positive for DCP. DCP positivity was associated with vascular invasion, tumor differentiation and size among patients with HCC, which was associated with albumin level among patients without HCC. Vitamin K was administered prior to transplantation to 20 patients who were positive for DCP (two with and 18 without HCC), resulting in a decrease in DCP levels in 19 of them.

*Conclusions:* Serum DCP levels may be raised in end-stage liver disease patients without HCC, and cannot be used as a reliable marker for HCC among liver transplant candidates.

**Key words:** hepatocellular carcinoma, sensitivity and specificity, tumor marker, vitamin K deficiency

## INTRODUCTION

CIRRHOSIS WITH EARLY-STAGE hepatocellular carcinoma (HCC) is currently one of the leading indications for liver transplantation. The introduction of the Milan criteria, i.e., a single tumor up to 5 cm in size or as many as three tumors up to 3 cm in size, and no vascular invasion has led to low incidence of recurrence post-transplantation in various transplant centers around the world.[1] The Milan criteria have now been adopted as the selection criteria for liver transplantation in the United States, Europe, and Japan.[2–4] Expanded criteria, such as the UCSF criteria or Tokyo rule, are proposed by several groups,[5,6] although the superiority of expanded criteria over Milan criteria is controversial.[7] Nevertheless, survival is reported to be poorer after liver transplantation for more advanced HCC outside the criteria, it is important to detect early-stage HCC that meets the eligibility requirements for liver transplantation.

In the screening for HCC, α-fetoprotein (AFP) measurement is widely used in conjunction with imaging studies, although the use of this marker alone has relatively low sensitivity (39–71%) and specificity (49–91%).[8,9] Other serum markers, such as des-γ-carboxy prothrombin (DCP) and the lens culinaris

*Correspondence: Dr Yasuhiko Sugawara, Department of Surgery, Artificial Organ and Transplantation Division, Graduate School of Medicine, The University of Tokyo, 7-3-1 Hongo, Bunkyo-ku, Tokyo 113-8655, Japan. Email: yasusuga-tky@umin.ac.jp*
*Received 20 March 2011; revision 17 June 2011; accepted 5 July 2011.*

**Table 1** Etiology of background liver diseases

| Etiology of background liver diseases | All patients ($n = 347$) | Histologically-confirmed HCC patients ($n = 106$) |
|---|---|---|
| HCV-related cirrhosis | 105 (30.3%) | 60 (56.6%) |
| HBV-related cirrhosis | 56 (16.1%) | 34 (32.0%) |
| HBV and HCV-related cirrhosis | 2 (0.6%) | 2 (1.8%) |
| Alcoholic liver cirrhosis | 4 (1.2%) | 4 (3.7%) |
| Cryptogenic cirrhosis† | 21 (6.1%) | 4 (3.7%) |
| Primary biliary cirrhosis | 69 (19.9%) | 2 (1.8%) |
| Primary sclerosing cholangitis | 10 (2.9%) | 0 |
| Autoimmune hepatitis | 12 (3.5%) | 0 |
| Biliary atresia | 18 (5.2%) | 0 |
| Metabolic disease | 11 (3.2%) | 0 |
| Fulminant hepatic failure | 32 (9.2%) | 0 |
| Others | 7 (2.0%) | 0 |

†History of alcohol intake and persistent HBV or HCV infection were denied in patients in this category.
HBV, hepatitis B virus; HCC, hepatocellular carcinoma; HCV, hepatitis C virus.

agglutinin-reactive fraction of AFP (AFP-L3), are also used in combination with AFP.[10–13] DCP is an abnormal prothrombin that is frequently increased in the serum of patients with HCC.[12,14] DCP was reported to be a more specific marker than AFP in early studies and meta-analysis, although a few recent studies showed contradicting results.[9,15–18] The combined use of AFP with DCP or AFP-L3 improves sensitivity and thus may contribute to early detection.[16,18–20]

Screening for HCC is usually not recommended among patients who are at advanced stage of cirrhosis unless curative treatment such as liver transplantation is readily available. In the United States, development of early HCC will give the patient a priority MELD score while patients are waiting for liver transplantation. Currently surveillance for HCC using ultrasonography with or without AFP measurement is recommended by the guideline of American Association for the Study of Liver Diseases.[2] However, no data to date suggest the use of DCP during pre-transplantation screening or diagnosis. Level of DCP in patients with severe liver impairment may be increased due to altered vitamin K metabolism such as obstructive jaundice or wide-spectrum antibiotics use.[19–23] If DCP levels often increase false-positively due to causes other than HCC, diagnostic accuracy of DCP will be reduced. In this study, we therefore aimed to evaluate the accuracy of AFP and DCP measurement for the diagnosis of HCC in liver transplant candidates, and to identify factors that contribute to elevated DCP levels.

## METHODS

### Patients

FROM JANUARY 1996 to December 2008, 347 adult-to-adult primary liver transplantations were performed at the University of Tokyo hospital. A retrospective review of records of all liver transplant recipients at the University of Tokyo was approved by the University of Tokyo Institutional Review Board (No. 2140). Of the 347 transplantations, 191 were performed in men and 156 in women. Median (range) age was 52 (18–67) years. Etiologies of the liver diseases are summarized in Table 1. Thirty-two patients with fulminant hepatic failure were excluded. The remaining 315 patients were included in the analysis. None of these patients were on warfarinization.

### Measurement of serum tumor markers

Serum tumor markers were measured routinely using a commercially available kit as a part of the pre-transplant evaluation; markers included were AFP, DCP, and carcinoembryonic antigen (CEA). Results obtained within one month prior to liver transplantation were considered to be valid data. If the test was repeated during this period, the highest value was adopted. Serum AFP and CEA levels were measured using an enzyme-linked immunoassay method until June 2001 and a fluorescence-enzyme immunoassay method thereafter. Commercially determined reference values were up to 9 ng/mL for AFP and up to 5.0 ng/mL for CEA. Of the

315 cases, 307 had valid AFP measurements and 299 cases valid CEA measurements within one month prior to liver transplantation. The median (range) levels of AFP and CEA were 8 (1–11 999) ng/mL and 4.1 (0.3–17.5) ng/nL, respectively. Serum DCP levels were measured using an enzyme-linked immunoassay (Eitest mono-P-II, or Eitest PIVKA-II kit, Sankyo Junyaku Co., Ltd, Tokyo, Japan) from 1996 to 2000. In 2000, we began using a Chemiluminescence assay (Picolumi PIVKA-II and Lumipluse, Sankyo Junyaku Co., Ltd, Tokyo). There were good correlations between the two measurement methods for DCP, with an $r$ between 0.98–0.99 (data provided by Sankyo Junyaku Co., Ltd. and Eisai Co., Ltd). The commercially determined reference value was <40 mAU/mL. There were 300 cases with valid data available with a median of 25 (3–36 613) mAU/mL. AFP-L3 was measured using lectin-affinity electrophoresis followed by antibody-affinity blotting,[24] and levels are shown as a percentage of total AFP. This test was performed in only a limited number of patients (99 patients in the HCC group and 17 patients in the non-HCC group) and thus the results were not included in the analysis.

## Imaging study prior to liver transplantation

Pre-transplant evaluation included multi-phase dynamic helical computed tomography (CT) with contrast enhancement taken within one month prior to liver transplantation. Images were reviewed by two independent radiologists; one of the radiologists was assigned to be a pre-transplant judge who was independent of the transplant surgical team (MA and KO). Protocol imaging examination was not performed in 25 of 315 recipients; films from the referral hospital were used in those cases. Nine patients underwent CT without contrast enhancement due to renal insufficiency; magnetic resonance imaging (MRI) and ultrasonography were used as adjunctive studies in such cases.

## Evaluation of the liver explants

Histopathologic findings of explanted livers were regarded as the gold standard in this study. Official histologic reports issued by pathologists were reviewed. Removed livers were sliced in approximately 1-cm thick sections along the axial plane to check for tumors on the cut surface. Pathologic features, including histologic differentiation, vascular invasion, and intrahepatic metastasis, were examined. If the histologic grade differed between nodules in the same liver, the worst grade was adopted in this study. The diameter of the largest tumor nodule was adopted as the "tumor size"; lesion by lesion analysis was not performed in this study. Explanted livers with known HCC were examined prospectively by *ex situ* ultrasound study.[25] Because the pathologists were not blinded, livers known to contain tumors might have been examined more carefully.

## Vitamin K administration

Our review of the patient charts indicated that vitamin K was administered in some cases. Physicians diagnosed patients with elevated DCP levels and a hemorrhagic tendency with a "coagulation disturbance due to vitamin K deficiency" and administered either vitamin K1 (phylloquinone 15 mg daily) or vitamin K2 (menatetrenone 20 mg daily). There was no uniform treatment protocol for the diagnosis of vitamin K deficiency; the durations of vitamin K treatment and repeat DCP measurements were determined by the treating physician.

## Statistical analysis

Data are presented as median and range or mean ± standard deviation for quantitative variables, unless otherwise specified. Differences between groups were analyzed by the Mann–Whitney $U$-test for continuous variables and the $\chi^2$ test for categorical variables. Log-normally distributed data were entered into analysis after log10 transformation. Two-tailed tests for significance were performed using a $P$-value of less than 0.05. Variables with a $P$-value of less than 0.05 were considered for entry into the multivariate logistic stepwise regression model. For the diagnostic performance of AFP and DCP, a receiver operating characteristics (ROC) curve was constructed and the area under the ROC curve (AUROC) was calculated. Data analysis was performed with SPSS version 12.0 (SPSS Inc., Chicago, IL, USA).

# RESULTS

## Patient characteristics

HEPATOCELLULAR CARCINOMAS MEETING Milan criteria were diagnosed prior to transplantation in 86 patients, exceeded the criteria in 15 patients, and was incidentally detected in the explanted liver in another five patients. In total, 106 patients were diagnosed with histologically confirmed HCC. Sixty-five patients had at least one history of treatment for HCC; percutaneous ethanol injection in 21, transcatheter arterial embolization in 49, radiofrequency ablation therapy in 13, and partial hepatic resection in 11. Of

**Table 2** Patient characteristics

| Factors | Valid data in analysis | Recipients with HCC ($n = 106$) | Recipients without HCC ($n = 209$) | *P*-value |
|---|---|---|---|---|
| Male gender | 315 | 87 (82%) | 87 (42%) | <0.001 |
| Age | 315 | 56 (40–67) | 50 (18–66) | <0.001 |
| Child class C | 297† | 35 (33%) | 156 (82%) | <0.001 |
| MELD score | 315 | 12 (6–34) | 14 (6–40) | 0.007 |
| Albumin (g/dl) | 315 | 2.8 (1.8–4.4) | 2.9 (1.5–4.4) | 0.92 |
| Total bilirubin (mg/dl) | 315 | 2.6 (0.3–36.3) | 7.0 (0.4–40.0) | <0.001 |
| AST (IU/ml) | 315 | 59 (18–281) | 78 (17–481) | <0.001 |
| Creatinine (mg/dl) | 315 | 0.7 (0.4–2.8) | 0.6 (0.2–4.6) | 0.001 |
| Prothrombin time (INR) | 315 | 1.59 (0.97–3.24) | 1.54 (0.87–7.48) | 0.71 |
| AFP (ng/ml) | 307 | 20 (1–11 999) | 3 (1–480) | <0.001 |
| DCP (mAU/ml) | 300 | 23 (7–10 592) | 25 (5–36 613) | 0.42 |
| CEA (ng/ml) | 299 | 5.4 (0.8–14.7) | 3.7 (0.3–17.5) | 0.001 |
| AFP-L3 (% of total AFP) | 116 | 0.5 (0.5–77.8) | 0.5 (0.5–35.7) | 0.092 |

†Patients with metabolic liver diseases, and other etiologies were excluded.
Data are presented as median and range or mean ± standard deviation.
AFP, α-fetoprotein; AFP-L3, L3 fraction of α-fetoprotein; AST, aspartate amino transferase; CEA, carcinoembryonic antigen; DCP, des-γ-carboxy prothrombin; HCC, hepatocellular carcinoma; INR, international normalized ratio; MELD, model for end stage liver disease.

those 106 patients, 65 (61%) met the Milan criteria by histologic evaluation. The number of tumors in the explanted livers was one in 35 (33.0%), two in 26 (24.5%), three in 13 (12.2%), and four or more in 32 (30.1%). The diameter of the largest tumor was 2.5 ± 1.5 cm. Histologic grade was well differentiated in 26 (24.5%), moderately differentiated in 63 (59.4%), poorly differentiated in six (5.6%), combined HCC and cholangiocellular carcinoma in one (0.9%), and necrotic tissue of HCC in 10 (9.4%). Vascular invasion was diagnosed in 21 (19.8%).

According to the histologic diagnosis of HCC, patients were divided into the HCC group ($n = 106$) or the non-HCC group ($n = 209$). The characteristics of the 315 recipients are summarized in Table 2. The HCC group was male dominant ($P < 0.001$), older in age ($P < 0.001$), and had lower model for end stage liver disease (MELD) scores ($P = 0.007$). AFP and CEA levels were significantly higher in the HCC group than in the non-HCC group, whereas DCP levels were similar between groups.

## Performance of AFP and DCP

A ROC curve for predicting histological presence of HCC was created for all patients (Fig. 1). The AUROC for AFP (0.83, 95% confidence interval (CI): 0.78–0.88) was larger than that for DCP (0.47, 95% CI: 0.41–0.54).

The AUROC did not change after removing 10 cases with necrotic HCC cells; the AUROC was 0.83 (95%CI: 0.79–0.88) for AFP and 0.48 (95% CI: 0.41–0.54) for DCP. Sensitivity and specificity of tumor markers with a commercially defined reference value of AFP ≥ 9 ng/mL and DCP ≥ 40 mAU/mL are shown in Table 3. We also

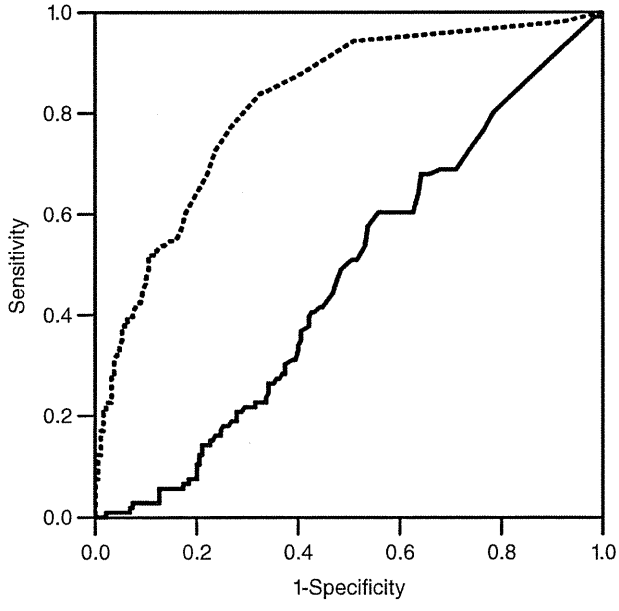


**Figure 1** The receiver operating characteristic curves for des-γ-carboxy prothrombin (DCP) (solid line) and α-fetoprotein (AFP) (dashed line) levels in the diagnosis of hepatocellular carcinoma (HCC) are shown.